

## Supporting Information

for *Adv. Sci.*, DOI 10.1002/adv.202406936

Targeting Neuraminidase 4 Attenuates Kidney Fibrosis in Mice

*Ping-Ting Xiao, Jin-Hua Hao, Yu-Jia Kuang, Cai-Xia Dai, Xiao-Ling Rong, Li-Long Jiang, Zhi-Shen Xie, Lei Zhang\*, Qian-Qian Chen\* and E-Hu Liu\**

**Supporting Information**

1 **Targeting Neuraminidase 4 Attenuates Kidney Fibrosis in Mice**

2

3 *Ping-Ting Xiao, Jin-Hua Hao, Yu-Jia Kuang, Cai-Xia Dai, Xiao-Ling Rong, Li-Long Jiang,*

4 *Zhi-Shen Xie, Lei Zhang<sup>\*</sup>, Qian-Qian Chen<sup>\*</sup>, E-Hu Liu<sup>\*</sup>*

5

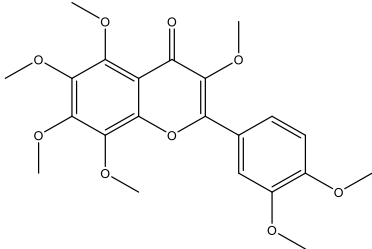
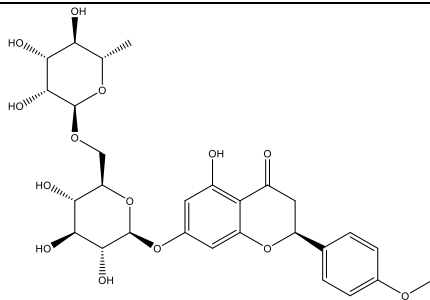
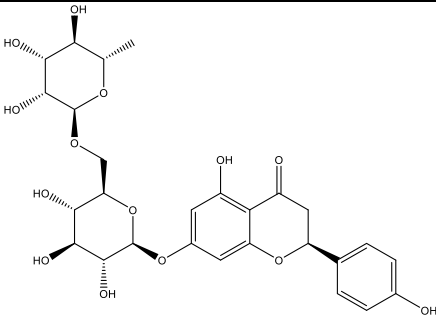
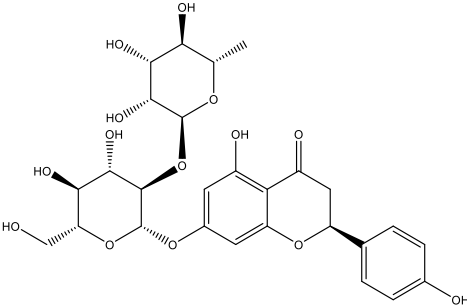
6

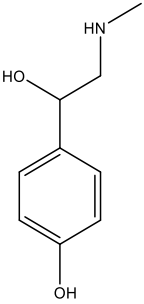
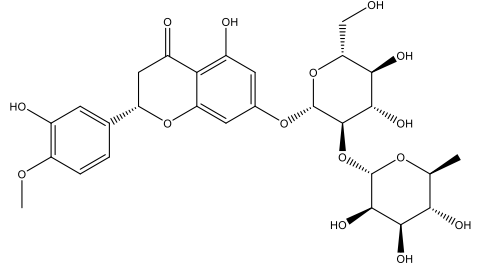
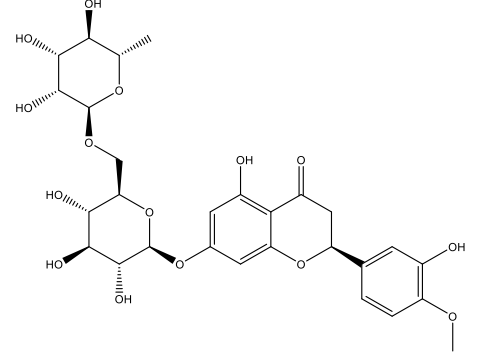
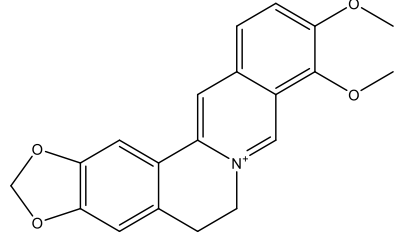
7 **Table S1** Clinical information of the subjects.

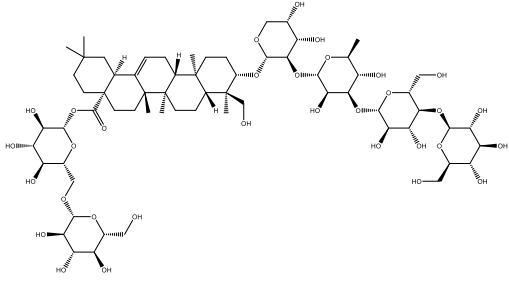
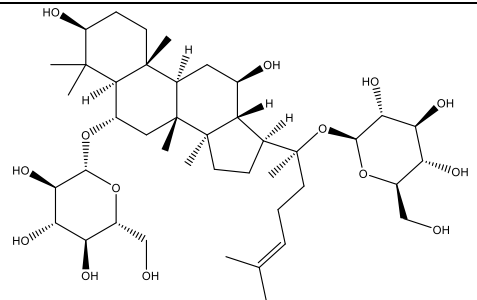
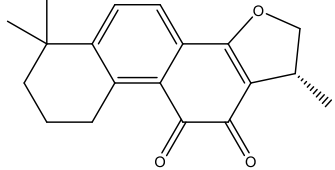
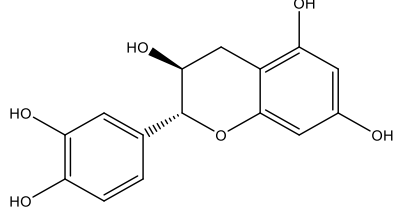
<b>Characteristics</b>	<b>Renal Fibrosis (<i>n</i> = 5)</b>	<b>Non-Renal Fibrosis (<i>n</i> = 4)</b>	<b><i>p</i> value</b>
Age (years)	41.6±12.7	23.25±10.3	0.05272
Male ( <i>n</i> , %)	3 (20%)	1 (25%)	0.35582
SCr (μmol/L)	212.96±60.03	54.5±12.71	0.001368
BUN (mmol/L)	9.38±3.92	3.65±0.98	0.025749
eGFR (mL/(min*1.73m <sup>2</sup> ))	30.79±9.26	129.34±17.21	3.71E-05
Comorbidities/Medical history			
Hypertension	3 (60%)	0	
Diabetes mellitus	0	0	
COPD or asthma	1 (25%)	0	
Coronary disease	0	0	
Morbid obesity	0	0	
Neurologic	1 (25%)	0	
Neoplasms (extra-renal)	0	0	

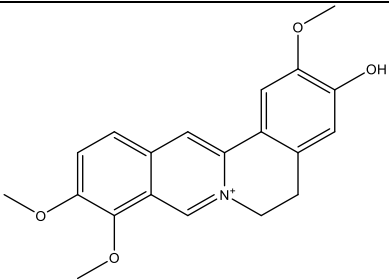
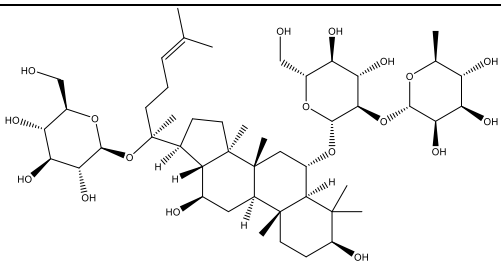
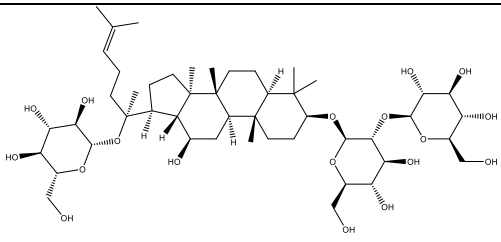
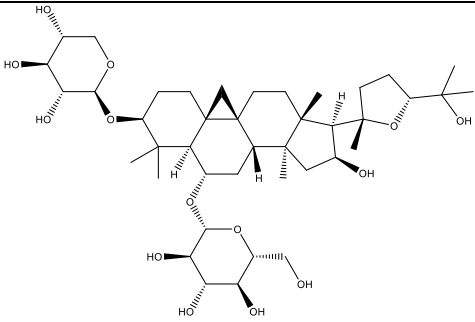
8 Unpaired two-tailed *t*-test. SCr: serum creatinine; BUN: Blood urea nitrogen. eGFR: Estimated glomerular filtration rate; COPD: chronic  
9 obstructive pulmonary disease.

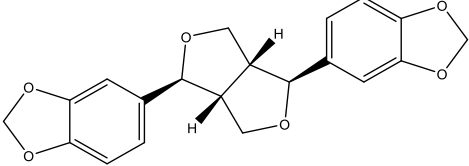
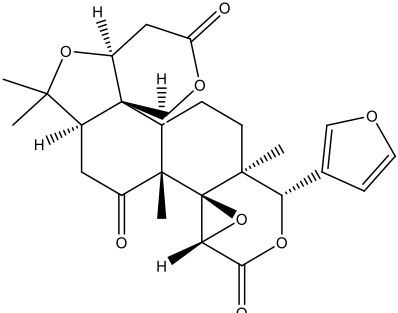
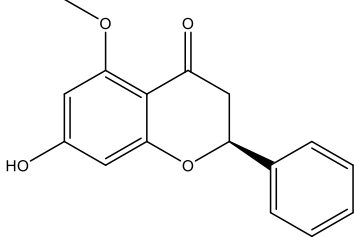
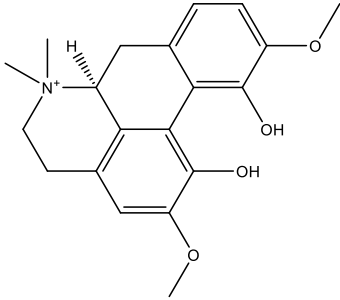
10 **Table S2** The inhibitory rate of 67 compounds on NEU4 enzyme activity.

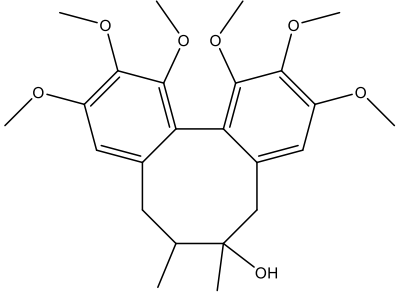
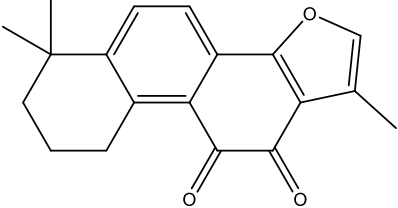
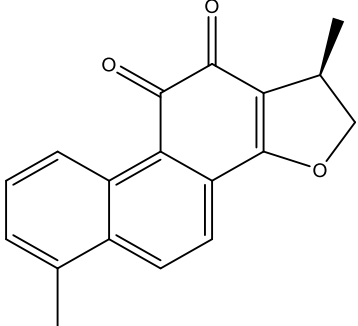
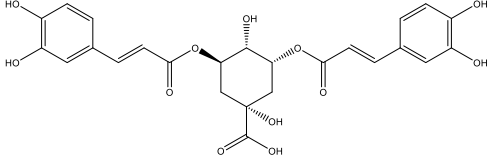
ID	Natural compound	Inhibition ratio±SD	Source	Structure
1	3,5,6,7,8,3',4'-Heptamethoxyflavone	44.6%±0.016	Biopurify Phytochemicals	
2	Didymin	10.9%±0.01	Biopurify Phytochemicals	
3	Narirutin	14.7%±0.023	Biopurify Phytochemicals	
4	Naringin	16.9%±0.03	Must bio-technology	

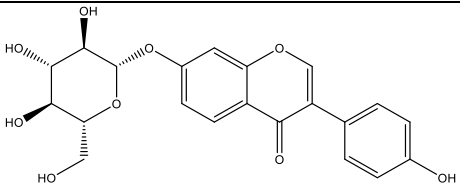
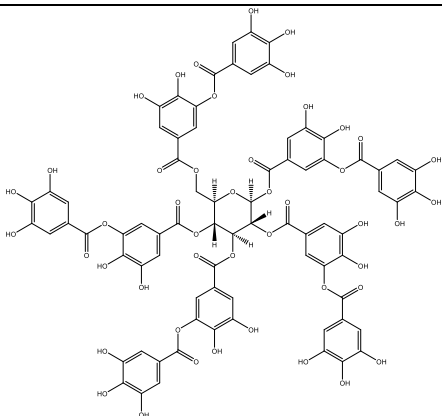
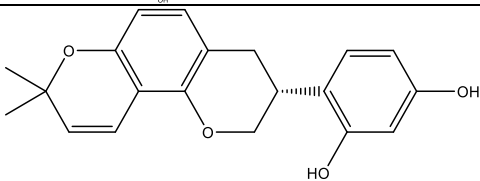
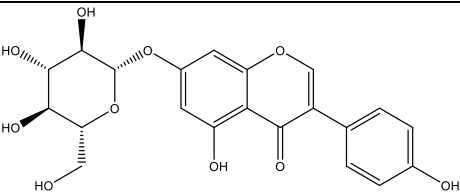
5	Synephrine	22.5%±0.074	Must bio-technology	
6	Neohesperidin	27.5%±0.009	Prepared in our laboratory	
7	Hesperidin	25.7%±0.013	Must bio-technology	
8	Berberine	15.6%±0.024	Must bio-technology	

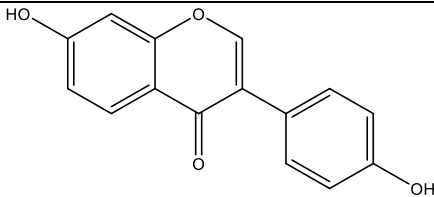
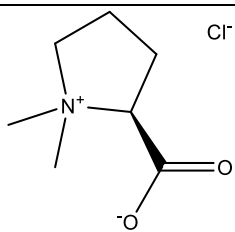
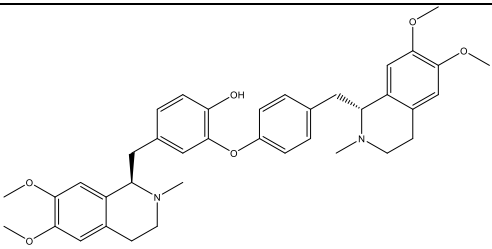
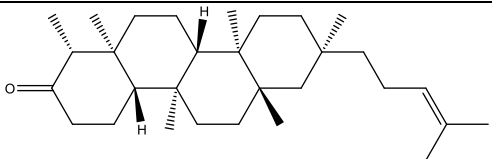
9	Macranthoidin B	6.4%±0.033	Must bio-technology	
10	Ginsenoside Rg1	2.1%±0.014	Must bio-technology	
11	Cryptotanshinone	6.4%±0.032	Must bio-technology	
12	Catechin	16.2%±0.008	Must bio-technology	

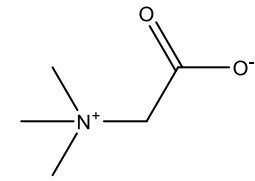
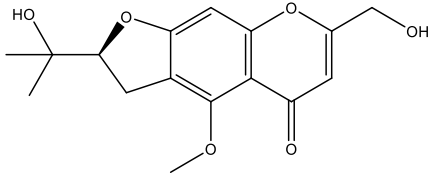
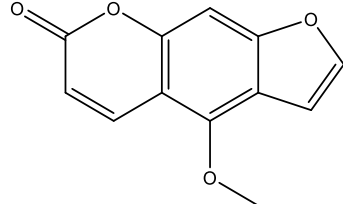
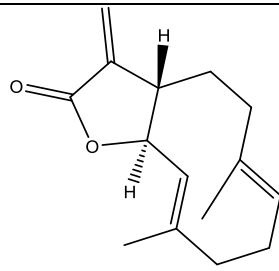
13	Jatrorrhizine	15.6%±0.04	Must bio-technology	
14	Ginsenoside Re	7.6%±0.012	Must bio-technology	
15	Ginsenoside Rd	11.3%±0.009	Must bio-technology	
16	Astragaloside A	10.5%±0.02	Must bio-technology	

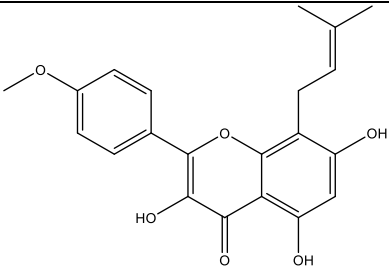
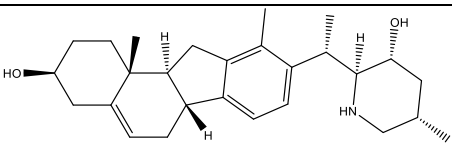
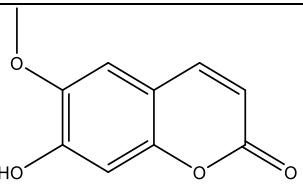
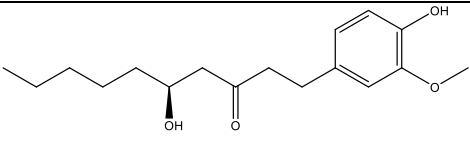
17	Sesamin	13.9%±0.018	Must bio-technology	
18	Limonin	10.6%±30.011	Must bio-technology	
19	Alpinetin	14.1%±0.04	Must bio-technology	
20	Magnoflorine	-182.4%±0.198	Must bio-technology	

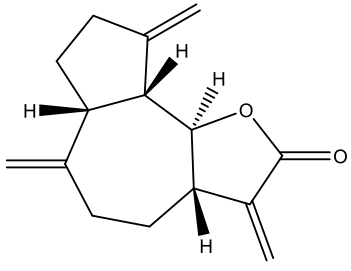
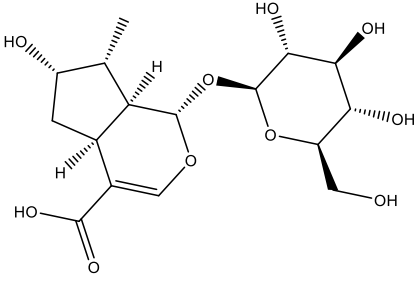
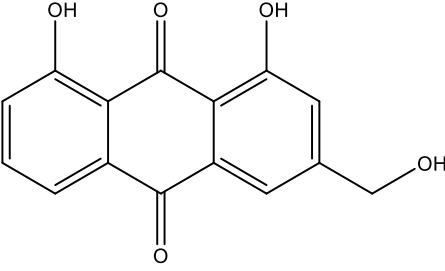
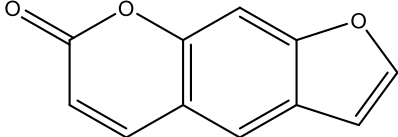
21	Schisandrin	7.4%±0.013	Must bio-technology	
22	Tanshinone II A	3.3%±0.013	Must bio-technology	
23	Dihydratanshinone I	17.5%±0.02	Must bio-technology	
24	Isochlorogenic acid A	39.5%±0.103	Must bio-technology	

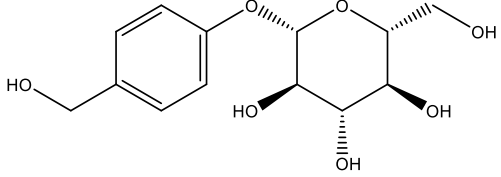
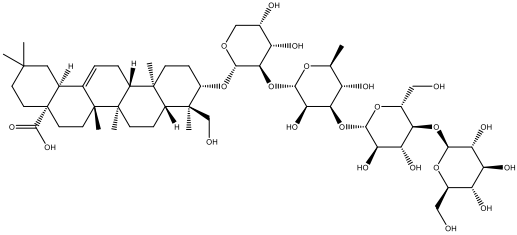
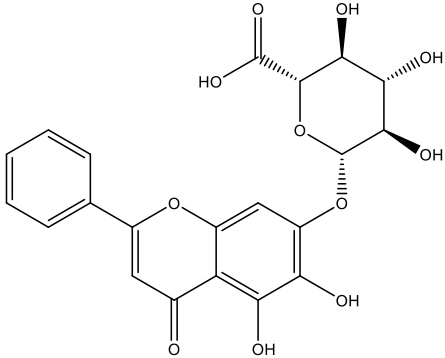
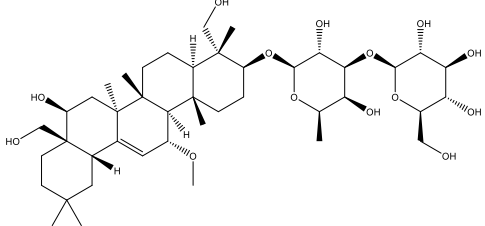
25	Daidzin	43.9%±0.036	Must bio-technology	
26	Tannic acid	-25.0%±0.03	Must bio-technology	
27	Glabridin	10.2%±0.038	Must bio-technology	
28	Genistin	19.3%±0.04	Must bio-technology	

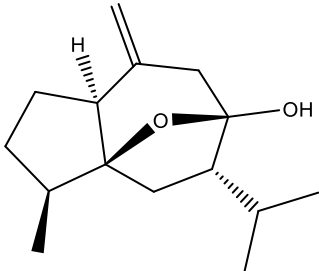
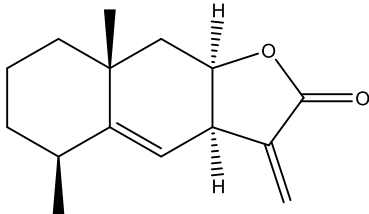
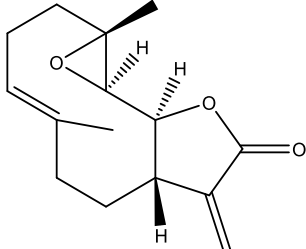
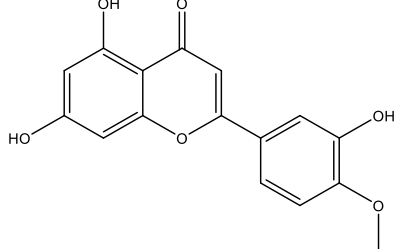
29	Daidzein	34.6%±0.053	Must bio-technology	
30	Stachydrine hydrochloride	4.9%±0.047	Must bio-technology	
31	Dauricine	29.9%±0.088	Must bio-technology	
32	Shionone	1.7%±0.059	Must bio-technology	

33	Betaine	2.8%±0.059	Must bio-technology	
34	Cimifugin	-24.9%±0.026	Must bio-technology	
35	Bergapten	23.3%±0.024	Must bio-technology	
36	Costunolide	15.2%±0.014	Must bio-technology	

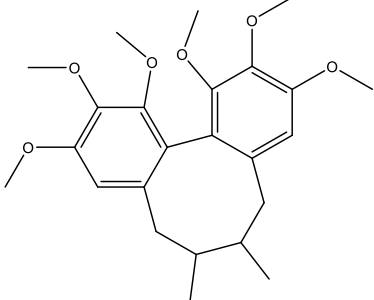
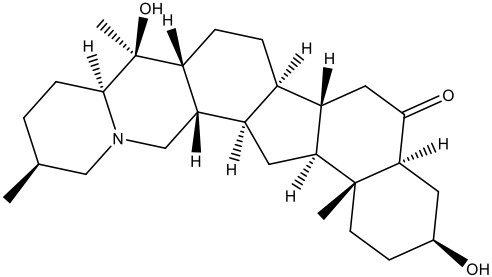
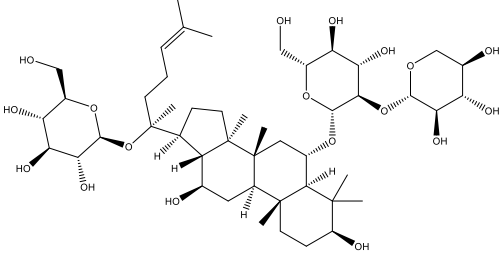
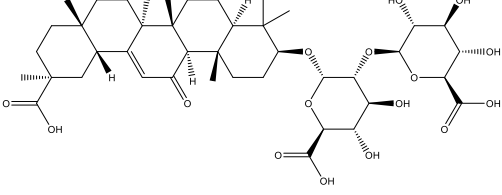
37	Icaritin	19.6%±0.022	Must bio-technology	
38	Veratramine	19.2%±0.011	Must bio-technology	
39	Scopoletin	-891.1%±0.242	Must bio-technology	
40	6-Gingerol	9.9%±0.032	Must bio-technology	

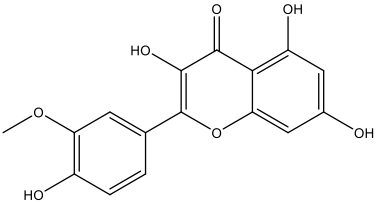
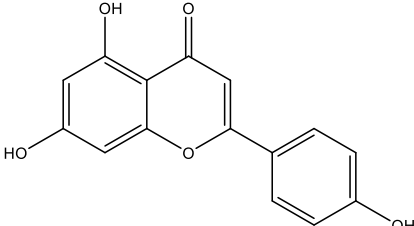
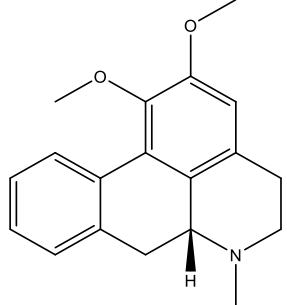
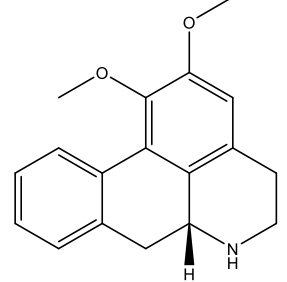
41	Dehydrocostus lactone	17.9%±0.019	Must bio-technology	
42	Loganic acid	-5.2%±0.012	Must bio-technology	
43	Aloe emodin	25.9%±0.208	Must bio-technology	
44	Psoralen	29.8%±0.012	Must bio-technology	

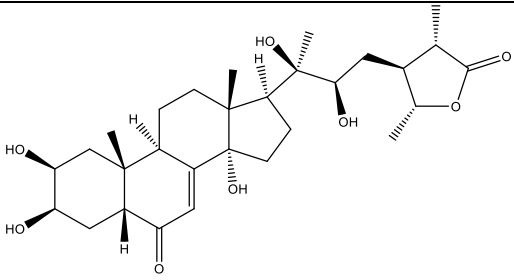
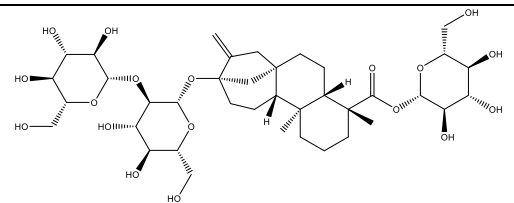
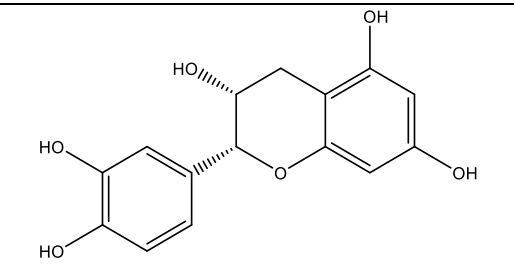
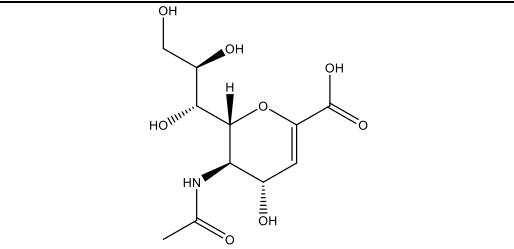
45	Gastrodin	3.6%±0.023	Must bio-technology	
46	Macranthoside B	10.9%±0.033	Must bio-technology	
47	Baicalin	32.1%±0.033	Must bio-technology	
48	Saikosaponin	3.9%±0.045	Must bio-technology	

49	Curcumol	6.9%±0.004	Must bio-technology	 <p>The structure of Curcumol is a complex polycyclic molecule. It features a central seven-membered ring containing an oxygen atom. This ring is fused to a five-membered ring on the left and a six-membered ring on the right. The six-membered ring has a methyl group on a wedge and a hydrogen on a dash. The seven-membered ring has a methyl group on a dash and a hydroxyl group on a wedge. A side chain with a terminal methyl group is attached to the seven-membered ring.</p>
50	Alantolactone	12.4%±0.021	Must bio-technology	 <p>The structure of Alantolactone is a bicyclic molecule consisting of a six-membered ring fused to a five-membered lactone ring. The six-membered ring has a methyl group on a wedge and a hydrogen on a dash. The lactone ring has a carbonyl group and a methyl group on a dash.</p>
51	Parthenolide	15.1%±0.014	Must bio-technology	 <p>The structure of Parthenolide is a complex polycyclic molecule. It features a central seven-membered ring containing an oxygen atom. This ring is fused to a six-membered ring on the left and a five-membered lactone ring on the right. The six-membered ring has a methyl group on a wedge and a hydrogen on a dash. The lactone ring has a carbonyl group and a methyl group on a dash.</p>
52	Diosmetin	17.5%±0.025	Must bio-technology	 <p>The structure of Diosmetin is a flavonoid molecule. It consists of a central chromone ring system. The 5-position of the chromone ring has a hydroxyl group, and the 7-position has a hydroxyl group. The 3-position of the chromone ring is substituted with a 4-methoxyphenyl group.</p>

53	Carnosic acid	35.2%±0.004	Must bio-technology	
54	Salidroside	1.1%±0.011	Must bio-technology	
55	Esculin	-1054.69%±12.193	Must bio-technology	
56	Evodiamine	-18.3%±0.087	Must bio-technology	

57	Deoxyschizandrin	1.4%±0.039	Must bio-technology	
58	Sipeimine	1%±0.01	Must bio-technology	
59	Notoginsenoside R1	-1.5%±0.008	Must bio-technology	
60	Glycyrrhizic acid	6.8%±0.019	Must bio-technology	

61	Isorhamnetin	22%±0.022	Must bio-technology	
62	Apigenin	27.8%±0.010	Must bio-technology	
63	Nuciferine	14.1%±0.018	Must bio-technology	
64	N-Nornuciferine	7.4%±0.042	Must bio-technology	

65	Cyasterone	6.3%±0.035	Must bio-technology	 <p>The structure of Cyasterone is a complex steroid molecule. It features a four-ring steroid nucleus with a ketone group at C-3 and a double bond at C-6. It has multiple hydroxyl groups at C-11, C-14, C-15, and C-20. A side chain at C-17 includes a methyl group, a hydroxyl group, and a branched chain ending in a hydroxyl group and a five-membered lactone ring.</p>
66	Stevioside	7.4%±0.014	Must bio-technology	 <p>The structure of Stevioside is a glycoside. It consists of a steviol aglycone core, which is a pentacyclic steroid with a methyl group at C-13 and a double bond at C-14. It is linked via an ester bond to a glucose molecule at C-13 and another glucose molecule at C-28. The glucose units are shown in their cyclic pyranose forms with various hydroxyl groups.</p>
67	Epicatechin	28.1%±0.027	Must bio-technology	 <p>The structure of Epicatechin is a flavan-3-ol. It features a chromane ring system with a benzene ring fused to a pyrogallane ring. The pyrogallane ring has hydroxyl groups at C-2 and C-3. The benzene ring has hydroxyl groups at C-5 and C-7. A hydroxyl group is also present at C-4 of the pyrogallane ring.</p>
68	2-deoxy-2,3-didehydro-N-acetylneuraminic acid	53.3%±0.017	TCI	 <p>The structure of 2-deoxy-2,3-didehydro-N-acetylneuraminic acid is a sialic acid derivative. It features a pyridine ring system with a hydroxyl group at C-4 and a double bond between C-2 and C-3. It has a hydroxyl group at C-5, an N-acetyl group at C-6, and a side chain at C-7 consisting of a hydroxyl group and a hydroxymethyl group.</p>

12 **Table S3** Nucleotide sequences of gene-specific primers used for quantitative real-time  
 13 reverse transcription PCR.

<b>Gene name</b>	<b>Primer</b>	<b>Sequence of primers (5' to 3')</b>
Human <i><math>\alpha</math>-SMA</i>	Forward	GCTGCCCAGAGACCCTGTT
	Reversed	TTTCATGGATGCCAGCAGACT
Human <i>VIMENTIN</i>	Forward	CAGAGAGAG GAAGCCGAAAG
	Reversed	ATGCTGTTCCTGAATCTGGG
Human <i>N-CADHERIN</i>	Forward	AAGAGAGACTGGGTCATCC
	Reversed	TGAGATGGGGTTGATAATG
Human <i>E-CADHERIN</i>	Forward	TAACAGGAACACAGGAGTCATCA
	Reversed	GTGGTGGGATTGAAGATCGG
Human <i>FNI</i>	Forward	CCACAGTGGAGTATGTGGTTAG
	Reversed	CAGTCCTTTAGGGCGATCAAT
Human <i>COL1A1</i>	Forward	TGTGCCACTCTGACTGGAAG
	Reversed	CGCCATACTCGAACTGGAATC
Human <i>COL3A1</i>	Forward	CGCCCTCCTAATGGTCAAGG
	Reversed	TTCTGAGGACCAGTAGGGCA
Human <i>COL4A1</i>	Forward	TGTTGACGGCTTACCTGGAGAC
	Reversed	GGTAGACCAACTCCAGGCTCTC
Human <i>CCL2</i>	Forward	CAGGTCCCTGTGTCATGCTTCT
	Reversed	GTCAGCACAGACCTCTCTCT
Human <i>PAIL</i>	Forward	GCACCACAGACGCGATCTT
	Reversed	ACCTCTGAAAAGTCCACTTGC
Human <i>TGF-<math>\beta</math></i>	Forward	CTAATGGTGGAAACCCACAACG
	Reversed	TATCGCCAGGAATTGTTGCTG
Human <i>ARG1</i>	Forward	TCAGAGCATGAGCGCCAAGT
	Reversed	CCTCGTGGCTGTCCCTTTGA
Human <i>NEU4</i>	Forward	GGCCACGGGATGACAGTTG
	Reversed	CAGGCGGATACCCATGTGTAG
Human <i>SNAIL</i>	Forward	TCGGAAGCCTAACTACAGCG
	Reversed	CAGATGAGCATTGGCAGCGA
Human <i>KIM-1</i>	Forward	CCCACGTCACCTATCGGAAG

	Reversed	GTGCTCAACACGGCAACAAT
Human <i>TNF<math>\alpha</math></i>	Forward	CCTCTCTCTAATCAGCCCTCTG
	Reversed	GAGGACCTGGGAGTAGATGAG
Human <i>IL6</i>	Forward	ACTCACCTCTTCAGAACGAATTG
	Reversed	CCATCTTTGGAAGGTTTCAGGTTG
Human <i>IL1<math>\beta</math></i>	Forward	AGCTACGAATCTCCGACCAC
	Reversed	CGTTATCCCATGTGTGCGAAGAA
Human <i>IL10</i>	Forward	ACCTGCCTAACATGCTTCGAG
	Reversed	GGCATCACCTCCTCCAGGTA
Human <i>P21</i>	Forward	TCTTGTACCCTTGTGCCTCG
	Reversed	ATCTGTCATGCTGGTCTGCC
Human <i>P16</i>	Forward	TGAAGCTCCCAGAATGCCAG
	Reversed	GCTGCCCTGGTAGGTTTTCT
Human <i>P53</i>	Forward	ACTTCAGGGGTGCCACATTC
	Reversed	CGACCCTGTCCCTCACCTCC
Human <i>IL8</i>	Forward	ACTCCAAACCTTTCCACCCC
	Reversed	CCTCTGCACCCAGTTTTCT
Human <i>KI67</i>	Forward	GGAAGCTGGACGCAGAAGAT
	Reversed	CAGCACCATTTGCCAGTTCC
Human $\gamma$ <i>H2AX</i>	Forward	AGAAGACGCGAATCATCCCC
	Reversed	TGGTCTTCTTGGGCAGCAG
Human <i>GAPDH</i>	Forward	GGAGCGAGATCCCTCCAAAAT
	Reversed	GGCTGTTGTCATACTTCTCATGG
Human $\beta$ - <i>actin</i>	Forward	GATCATTGCTCCTCCTGAGC
	Reversed	ACTCCTGCTTGCTGATCCAC
Mouse $\alpha$ - <i>Sma</i>	Forward	GGACTTTGAAAATGAGATGG
	Reversed	TGATGCTGTTATAGGTGGTT
Mouse <i>Vimentin</i>	Forward	CAGAGAGAG GAAGCCGAAAG
	Reversed	ATGCTGTTCCCTGAATCTGGG
Mouse <i>N-cadherin</i>	Forward	AAGAGAGACTGGGTCATCC
	Reversed	TGAGATGGGGTTGATAATG
Mouse <i>Fibronectin</i>	Forward	CCACAGTGGAGTATGTGGTTAG

---

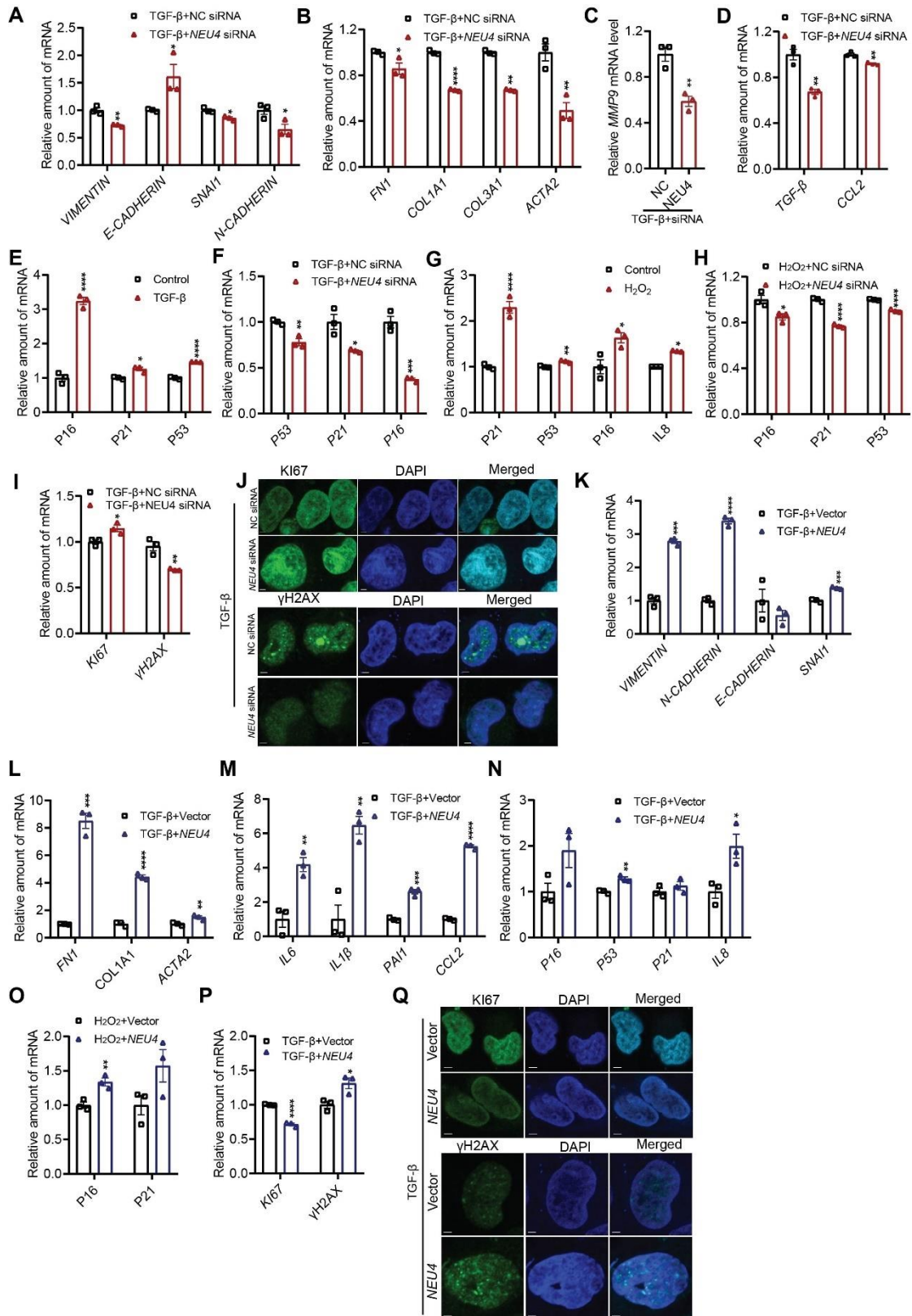
	Reversed	CAGTCCTTTAGGGCGATCAAT
Mouse <i>Kim-1</i>	Forward	CTATGTTGGCATCTGCATCG
	Reversed	AAGGCAACCACGCTTAGAGA
Mouse <i>Neu4</i>	Forward	GAACAGCGACTTAGCCCTGATG
	Reversed	TAGACCTGTGCTCCTCCAGTAC
Mouse <i>Snai1</i>	Forward	CTCCAAACCCACTCGGATGT
	Reversed	AGCCAGACTCTTGGTGCTTG
Mouse <i>Snai2</i>	Forward	GCCTCCAAGAAGCCCAACTA
	Reversed	GCCGACGATGTCCATACAGT
Mouse <i>E-cadherin</i>	Forward	TAACAGGAACACAGGAGTCATCA
	Reversed	GTGGTGGGATTGAAGATCGG
Mouse <i>Coll1a1</i>	Forward	TTGGAGAGAGCATGACCG
	Reversed	TACGCTGTTCTTGCAGTG
Mouse <i>Col3a1</i>	Forward	GTCTGGTGGCTTTTCACCCT
	Reversed	AGTTCGGGGTGGCAGAATTT
Mouse <i>Col4a1</i>	Forward	AACAACGTCTGCAACTTCGC
	Reversed	CTTCACAAACCGCACACCTG
Mouse <i>Ccl2</i>	Forward	CAGGTCCCTGTCATGCTTCT
	Reversed	GTCAGCACAGACCTCTCTCT
Mouse <i>Tgf-β</i>	Forward	GACCGCAACAACGCCATCTA
	Reversed	GGCGTATCAGTGGGGGTCAG
Mouse <i>Mmp2</i>	Forward	ACCTGAACACTTTCTATGGCTG
	Reversed	CTTCCGCATGGTCTCGATG
Mouse <i>Mmp7</i>	Forward	TAGGCGGAGATGCTCACTTT
	Reversed	TTCTGAATGCCTGCAATGTC
Mouse <i>Mmp9</i>	Forward	CTGGACAGCCAGACACTAAAG
	Reversed	CTCGCGGCAAGTCTTCAGAG
Mouse <i>Mmp13</i>	Forward	CTGGTCTTCTGGCACACGCT
	Reversed	GCAGCGCTCAGTCTCTTCAC
Mouse <i>Fsp1</i>	Forward	TGAGCAACTTGGACAGCAACA
	Reversed	TTCCGGGGTTCCTTATCTGGG
Mouse <i>Timp1</i>	Forward	GCAACTCGGACCTGGTCATAA

---

---

	Reversed	CGGCCCGTGATGAGAACT
Mouse <i>Tnfa</i>	Forward	TCTCATGCACCACCATCAAGGACT
	Reversed	ACCACTCTCCCTTTGCAGAATCA
Mouse <i>Il6</i>	Forward	ATCCAGTTGCCTTCTTGGGACTGA
	Reversed	TAAGCCTCCGACTTGTGAAGTGGT
Mouse <i>Il1β</i>	Forward	GCAACTGTTCCTGAACTCAACT
	Reversed	ATCTTTTGGGGTCCGTCAACT
Mouse <i>Yap</i>	Forward	CCAGACGACTTCCTCAACAGTG
	Reversed	GCATCTCCTTCCAGTGTGCCAA
Mouse <i>Negr1</i>	Forward	GCCTTCGAGTGGTACAAAGGA
	Reversed	CTGTACTTGGAGGGTTGAGGG
Mouse <i>Ankrd1</i>	Forward	ATAAACGGACGGCACTCCAC
	Reversed	CATCTGCGTTTCCCTCCACGA
Mouse <i>Ctgf</i>	Forward	GCCTACCGACTGGAAGACAC
	Reversed	GTA ACTCGGGTGGAGATGCC
Mouse <i>Cyr61</i>	Forward	ATGACCTCCTCGGACTCGAT
	Reversed	GGGTTGAAAAGA ACTCGCGG
Mouse <i>P21</i>	Forward	TTGTCGCTGTCTTGC ACTCT
	Reversed	TTTCGGCCCTGAGATGTTCC
Mouse <i>P16</i>	Forward	GAACTCTTTCGGTTCGTACCCC
	Reversed	TAGTGGGGTCCCTCGCAGTT
Mouse <i>P53</i>	Forward	TGGAGGAGTCACAGTCGGAT
	Reversed	CGTCCATGCAGTGAGGTGAT
Mouse <i>Il8</i>	Forward	TGGGTGAAGGCTACTGTTGG
	Reversed	AGCTTCATTGCCGGTGGAAA
Mouse <i>GAPDH</i>	Forward	TGTGTCCGTCGTGGATCTGA
	Reversed	CCTGCTTCACCACCTTCTTGAT
Mouse <i>β-actin</i>	Forward	GCTCTGGCTCCTAGCACC
	Reversed	CCACTATCCACACAGAGTACTTG

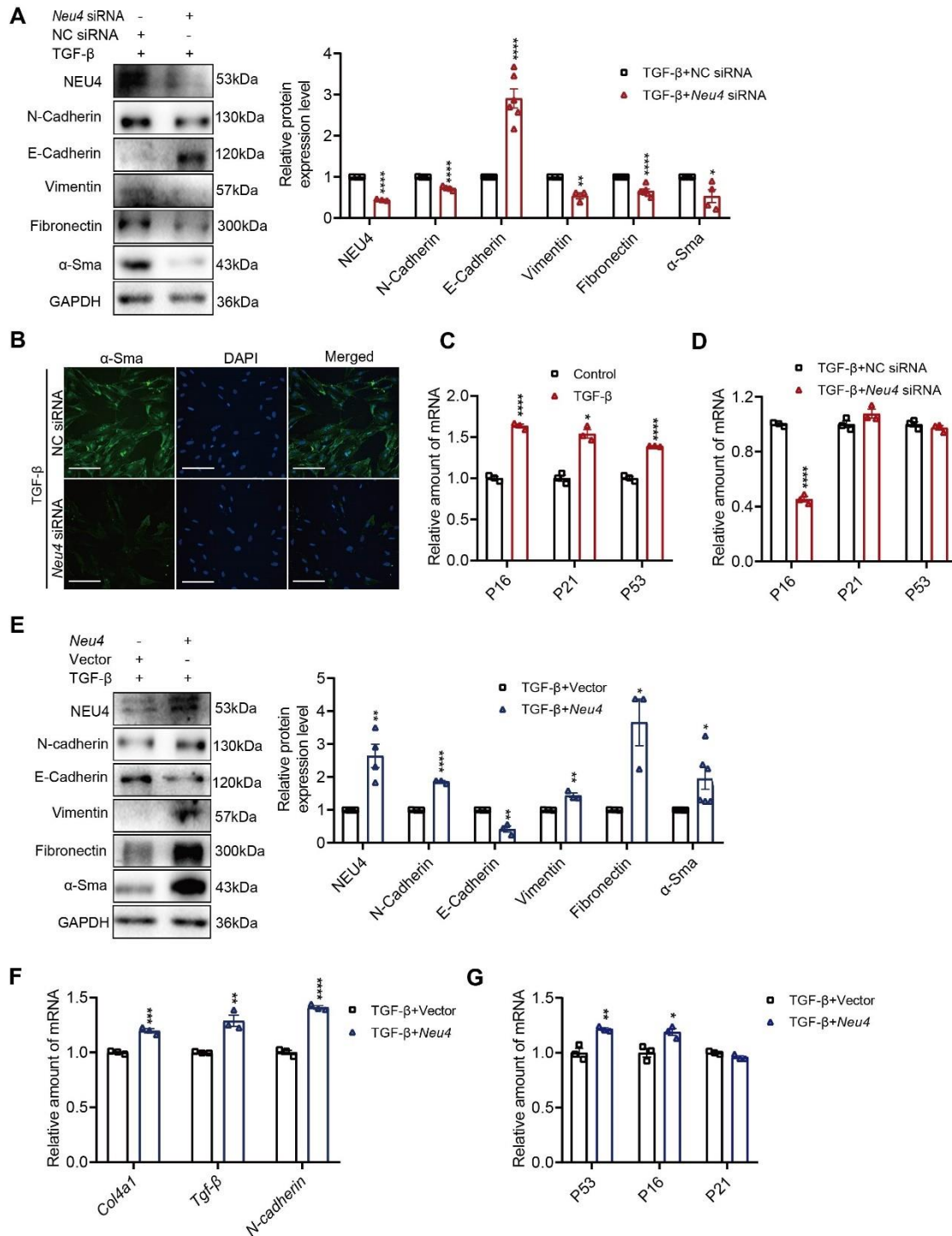
---



15

16 **Figure S1. NEU4 promoted epithelial-mesenchymal transition (EMT) and cellular**  
 17 **senescence in TGF-β-induced HK-2 cells. (A-F, I) Relative EMT associated gene (A),**  
 18 **ECM associated gene (B), *MMP9* (C), chemokine associated (D), senescence-**

19 associated gene (**E, F**) and DNA damage marker gene (**I**) mRNA level in HK-2 cells. *n*  
20 = 3 samples. (**G, H**) Relative senescence-associated gene mRNA level in HK-2 cells. *n*  
21 = 3 samples. (**J, Q**) Immunofluorescent staining represents KI67 or  $\gamma$ H2AX in HK-2  
22 cells. Scale bar, 10  $\mu$ m, *n* = 3 samples. (**K-P**) Relative EMT associated gene (**K**), ECM  
23 associated gene (**L**), inflammation associated gene (**M**), senescence-associated gene (**N**,  
24 **O**) and DNA damage marker gene (**P**) mRNA level in HK-2 cell. *n* = 3 samples. (**A-D**,  
25 **F, I, J**) HK-2 cells treatment with TGF- $\beta$  24 h after transfection with *NEU4* siRNA. (**E**,  
26 **G**) HK-2 cells treatment with TGF- $\beta$  24 h or H<sub>2</sub>O<sub>2</sub> 6 h. (**K-Q**) HK-2 cells treatment  
27 with TGF- $\beta$  24 h after transfection with *NEU4*-overexpression plasmids. (**H, O**) HK-2  
28 cells treatment with H<sub>2</sub>O<sub>2</sub> 6 h after transfection with *NEU4* siRNA (**H**) or *NEU4*-  
29 overexpression plasmids (**O**). Data are presented as mean  $\pm$  SEM. Comparisons  
30 between two groups were analyzed by using a two-tailed Student's *t* test. \**p*<0.05,  
31 \*\**p*<0.01, \*\*\**p*<0.001, \*\*\*\**p*<0.0001 versus the NC siRNA or Vector group.

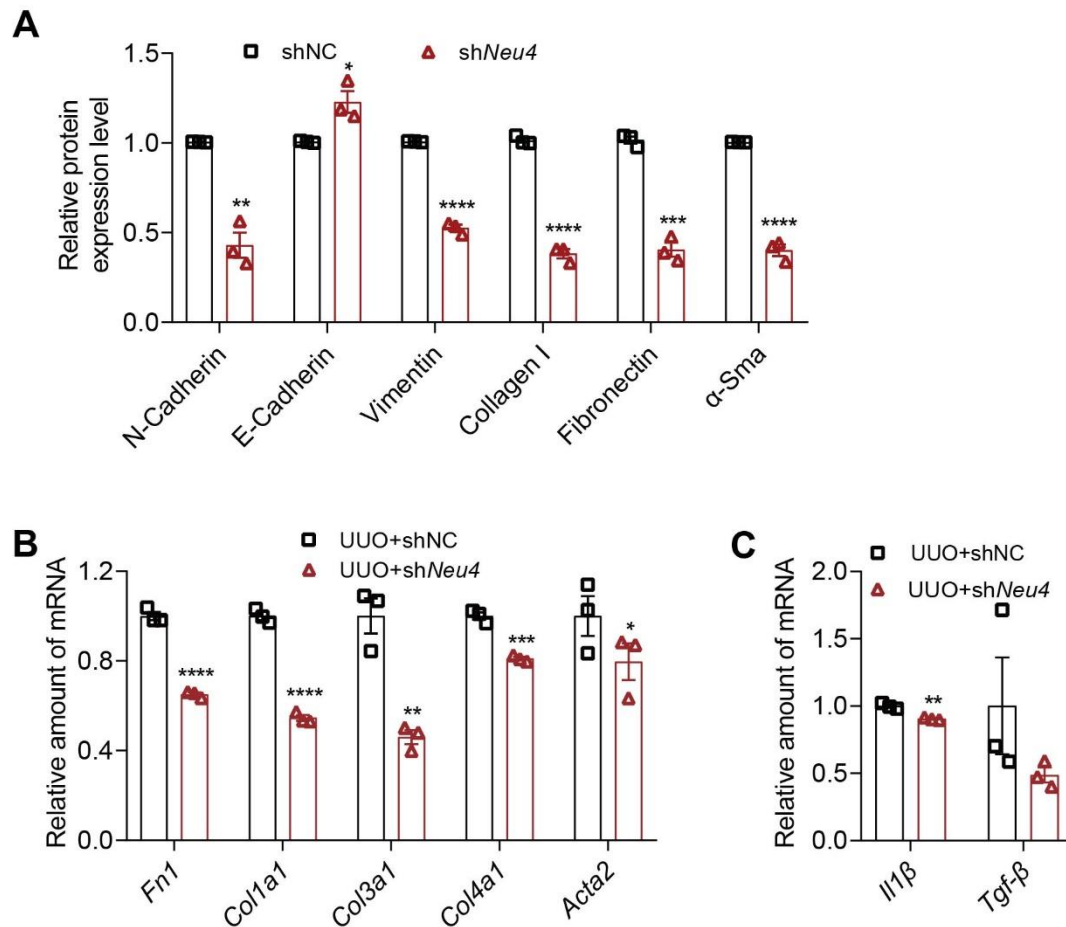


32

33 **Figure S2. NEU4 promoted EMT and cell senescence in TGF- $\beta$ -induced PTECs.**

34 (A) Western blot (left panel) and quantification (right panel) of the protein expression  
 35 of NEU4, N-Cadherin, E-Cadherin, Vimentin, Fibronectin and  $\alpha$ -Sma in PTECs.  
 36 GAPDH served as loading control,  $n = 3-6$  samples. (B) Immunofluorescent staining  
 37 represents  $\alpha$ -Sma in PTECs. Scale bar, 100  $\mu$ m,  $n = 3$  samples. (C, D) Relative  
 38 senescence associated gene mRNA level in PTECs,  $n = 3$  samples. (E) Western blot

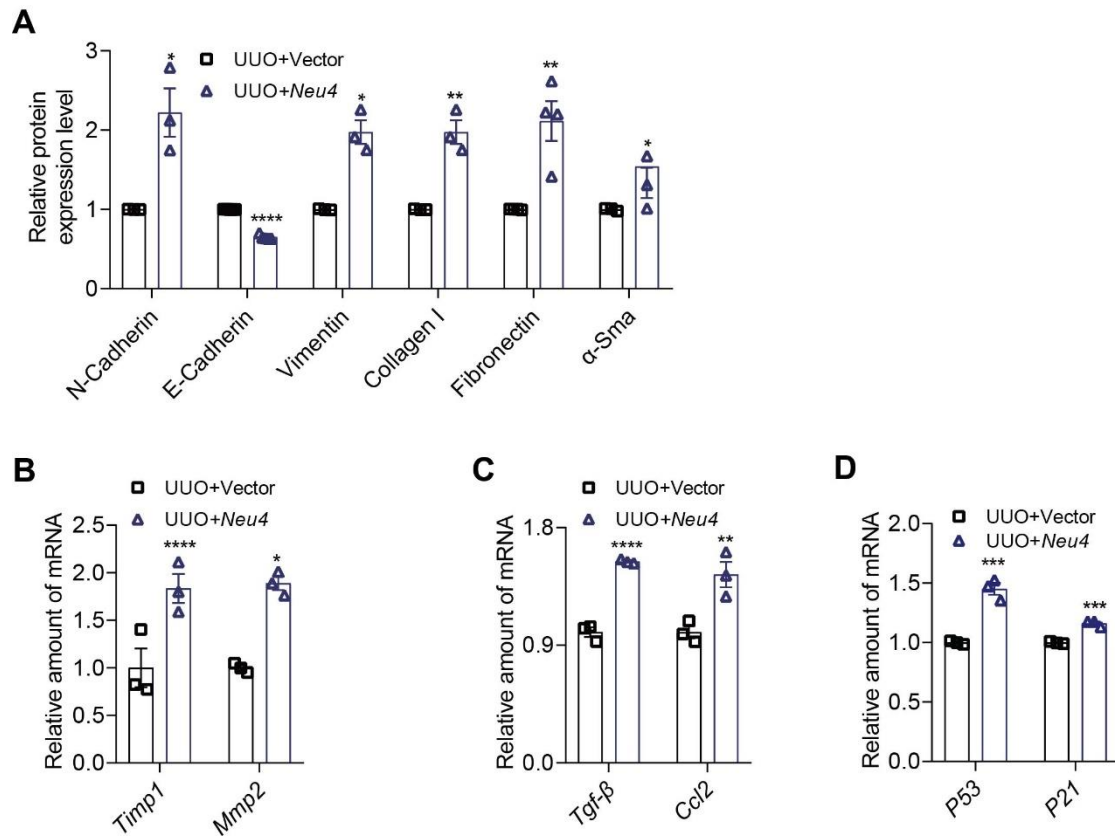
39 (left panel) and quantification (right panel) of the protein expression of NEU4, N-  
40 Cadherin, E-Cadherin, Vimentin, Fibronectin and  $\alpha$ -Sma in PTECs. GAPDH served as  
41 loading control,  $n = 3-6$  samples. **(F, G)** Relative EMT associated gene, ECM associated  
42 gene **(F)** and senescence associated gene **(G)** mRNA level in PTECs,  $n = 3$  samples. **(C)**  
43 PTECs treatment with TGF- $\beta$  24 h. **(A-B, D)** PTECs treatment with TGF- $\beta$  24 h after  
44 transfection with *Neu4* siRNA. **(E-G)** PTECs treatment with TGF- $\beta$  24 h after  
45 transfection with *Neu4*-overexpression plasmids. Error bars represent mean  $\pm$  SEM.  
46 Comparisons between two groups were analyzed by using a two-tailed Student's *t* test.  
47 \* $p < 0.05$ , \*\* $p < 0.01$ , \*\*\* $p < 0.001$ , \*\*\*\* $p < 0.0001$  versus the NC siRNA or Vector group.  
48



49

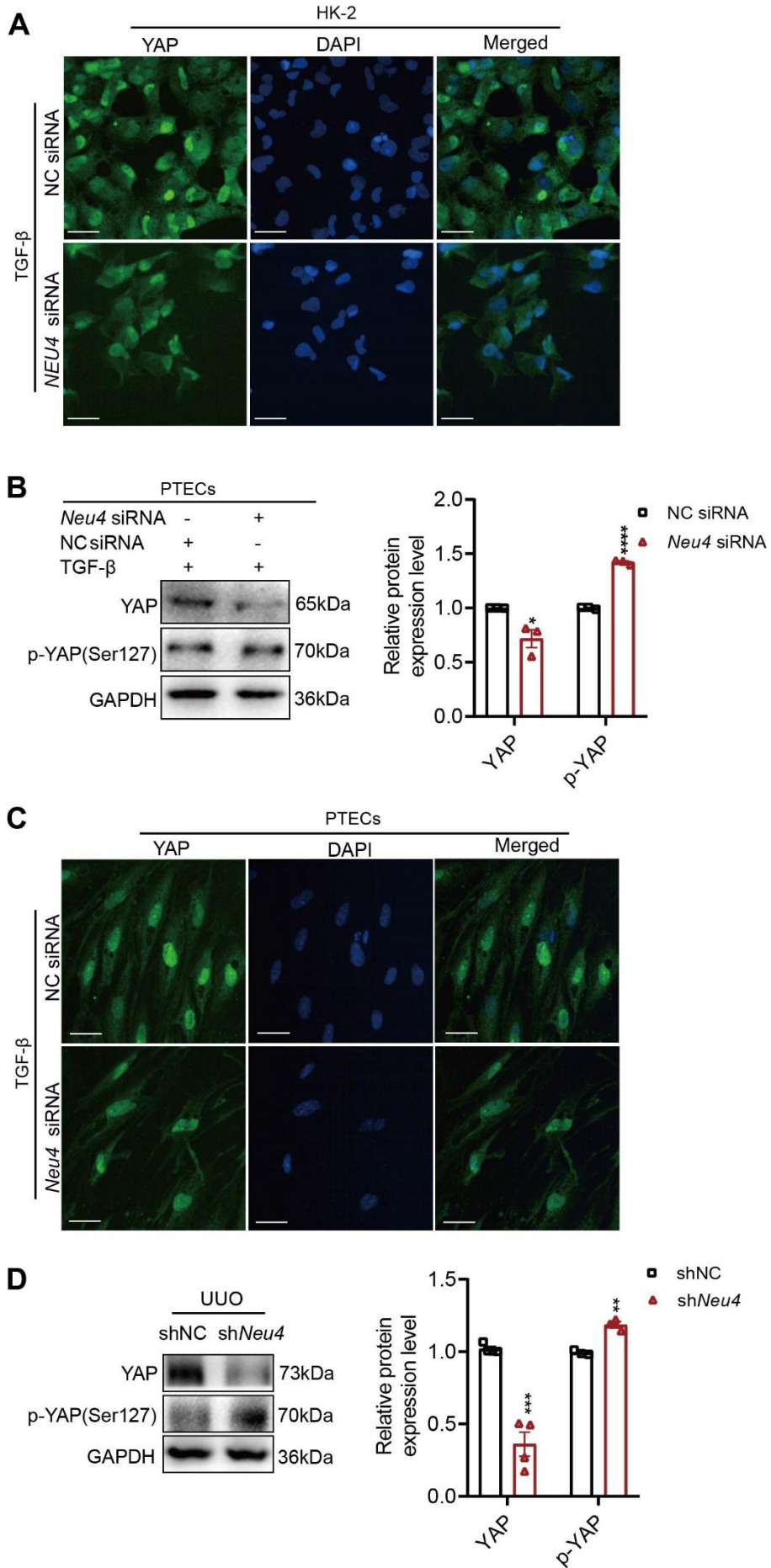
50 **Figure S3. *Neu4* knockdown alleviated UO-induced EMT, ECM and**  
 51 **inflammation in mice.** (A) Quantification of the expression of N-Cadherin, E-  
 52 Cadherin, Vimentin, Collagen I, Fibronectin and  $\alpha$ -Sma as shown in Figure 3E.  
 53 GAPDH served as loading control.  $n = 3-5$  mice. (B, C) Relative mRNA level of ECM  
 54 associated genes (B) and inflammation associated genes (C) were determined by RT-  
 55 qPCR,  $n = 3$  mice. Error bars represent mean  $\pm$  SEM. Comparisons between two groups  
 56 were analyzed by using a two-tailed Student's  $t$  test. \* $p < 0.05$ , \*\*\*\* $p < 0.0001$  versus the  
 57 shNC.

58



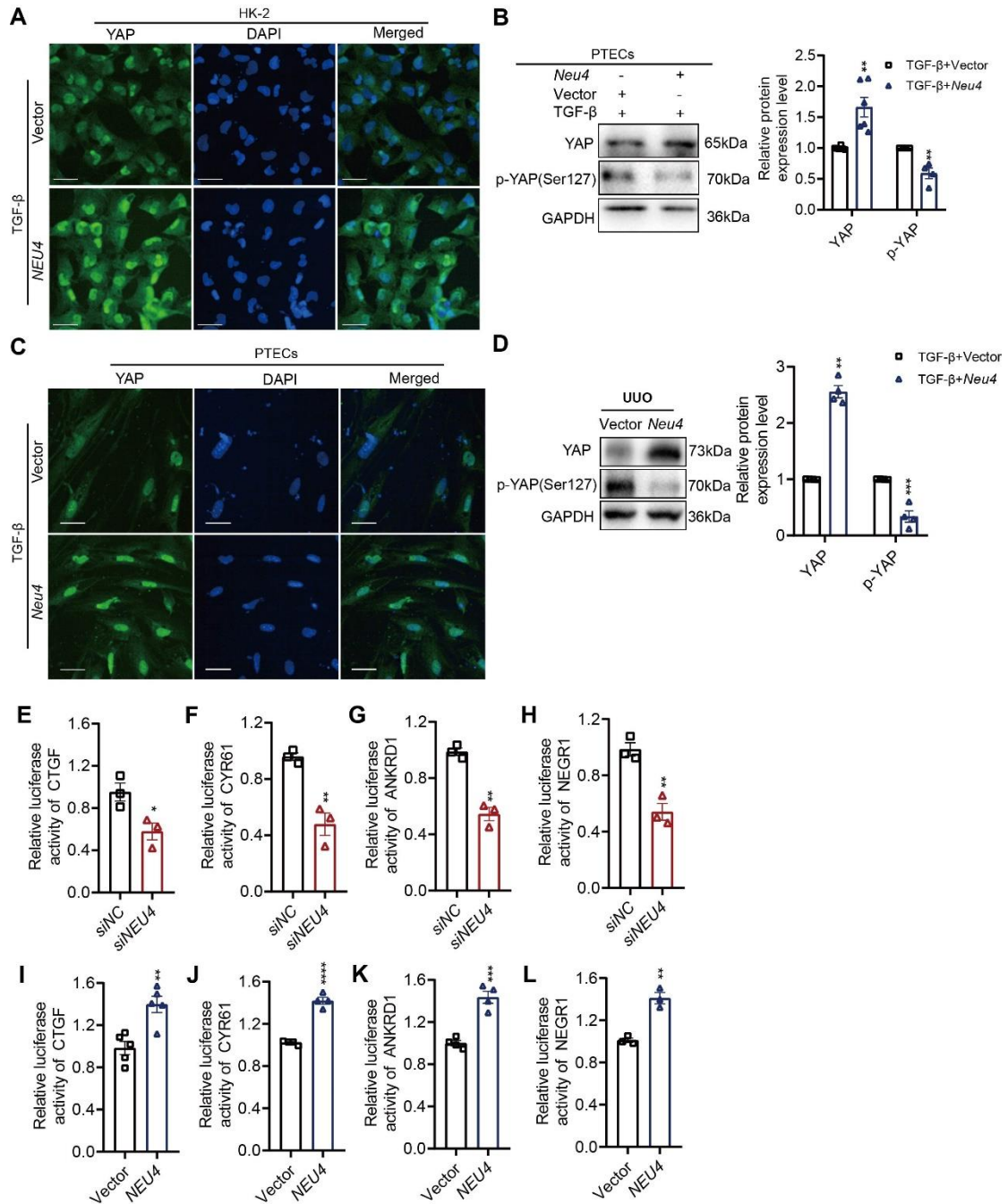
59

60 **Figure S4. Neu4 overexpression aggravated UO-induced EMT and cellular**  
 61 **senescence in mice. (A)** Quantification of the protein expression of  $\alpha$ -Sma, N-Cadherin,  
 62 E-Cadherin, Vimentin, Fibronectin and Collagen I in kidneys as shown in Figure 4E.  
 63 GAPDH served as loading control,  $n = 3-5$  mice. **(B-D)** Relative extracellular matrix  
 64 associated gene **(B)**, chemokine associated **(C)** and senescence associated gene **(D)**  
 65 mRNA level in left kidney.  $n = 3$  mice. Error bars represent mean  $\pm$  SEM. Comparisons  
 66 between two groups were analyzed by using a two-tailed Student's  $t$  test. \* $p < 0.05$ ,  
 67 \*\* $p < 0.01$ , \*\*\* $p < 0.001$ , \*\*\*\* $p < 0.0001$  versus the Vector group.



69 **Figure S5. NEU4 knockdown inhibits activation of Yes-associated protein (YAP).**  
70 **Related to Figure 6. (A)** Immunofluorescent staining represents YAP in HK-2 cells  
71 treatment with TGF- $\beta$  24 h after transfection with *Neu4* siRNA. Scale bar, 100  $\mu$ m,  $n$  =  
72 3 samples. **(B)** Western blot (left panel) and quantification (right panel) of the protein  
73 expression of YAP and phosphorylation of YAP in PTECs. GAPDH served as loading  
74 control,  $n$  = 3 samples. **(C)** Immunofluorescent staining represents YAP in PTECs.  
75 Scale bar, 100  $\mu$ m,  $n$  = 3 samples. **(D)** Western blot (left panel) and quantification (right  
76 panel) of the protein expression of YAP and phosphorylation of YAP in left kidneys  
77 from UUO mice with sh*Neu4*. GAPDH served as loading control,  $n$  = 3-4 mice. **(B and**  
78 **C)** PTECs treatment with TGF- $\beta$  24 h after transfection with *Neu4* siRNA. Error bars  
79 represent mean  $\pm$  SEM. Comparisons between two groups were analyzed by using a  
80 two-tailed Student's *t* test. \* $p$ <0.05, \*\* $p$ <0.01, \*\*\* $p$ <0.001, \*\*\*\* $p$ <0.0001 versus the  
81 NC siRNA or shNC group.

82



83

84 **Figure S6. NEU4 overexpression promotes activation of YAP.** (A)

85 Immunofluorescent staining represents YAP in HK-2 cells treatment with TGF-β 24 h

86 after transfection with *NEU4*-overexpression plasmids. Scale bar, 100 μm, *n* = 3

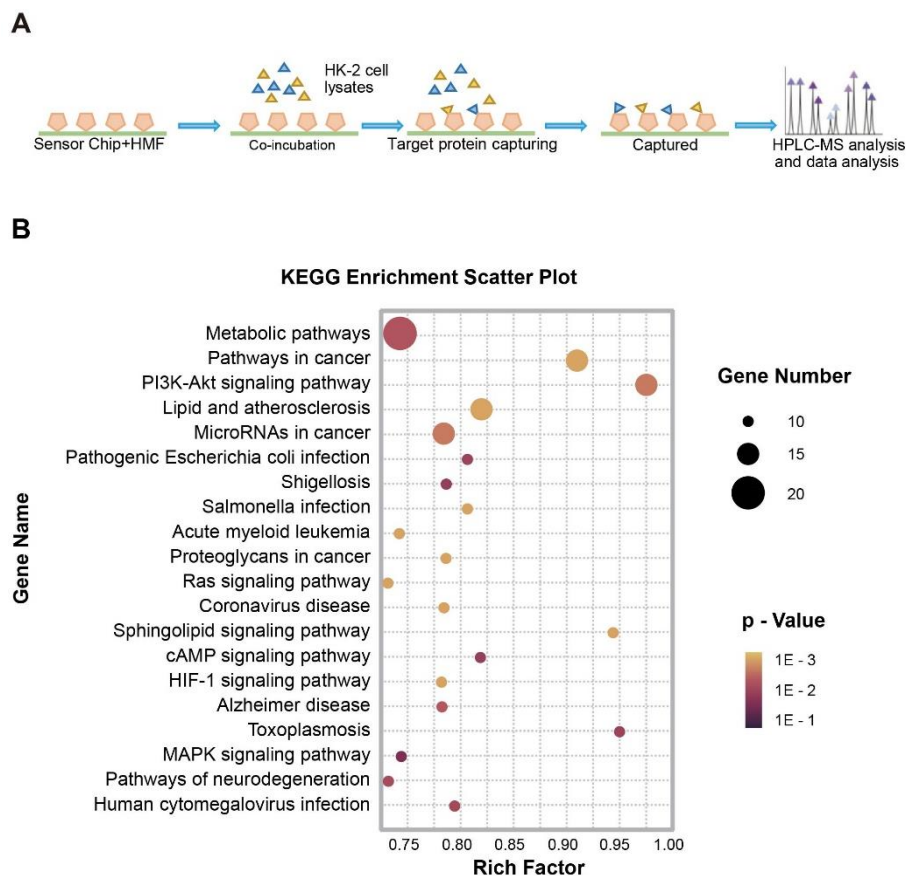
87 samples. (B) Western blot (left panel) and quantification (right panel) of YAP and

88 phosphorylation of YAP in PTECs, GAPDH served as loading control, *n* = 4-6 samples.

89 (C) Immunofluorescent staining represents YAP in PTECs. Scale bar, 100 μm, *n* = 3

90 samples. (D) Western blot (left panel) and quantification (right panel) of the protein

91 expression of YAP and phosphorylation of YAP in left kidneys from UUO mice with  
92 *Neu4*-overexpression plasmids. GAPDH served as loading control,  $n = 4$  mice. (**B** and  
93 **D**) PTECs treatment with TGF- $\beta$  24 h after transfection with *Neu4*-overexpression  
94 plasmids. (**E-L**) 293T cells were co-transfected with *YAP* and *Luc-CTGF* or *Luc-CYR61*  
95 or *Luc-ANKRD1* or *Luc-NEGR1* and si*NEU4* (E-H) or *NEU4* plasmid (I-L) for 48 h.  
96 Luciferase activity was determined using the luciferase reporter system.  $n = 3-5$  samples.  
97 Error bars represent mean  $\pm$  SEM. Comparisons between two groups were analyzed by  
98 using a two-tailed Student's *t* test. \* $p < 0.05$ , \*\* $p < 0.01$ , \*\*\* $p < 0.001$ , \*\*\*\* $p < 0.0001$   
99 versus the Vector group.



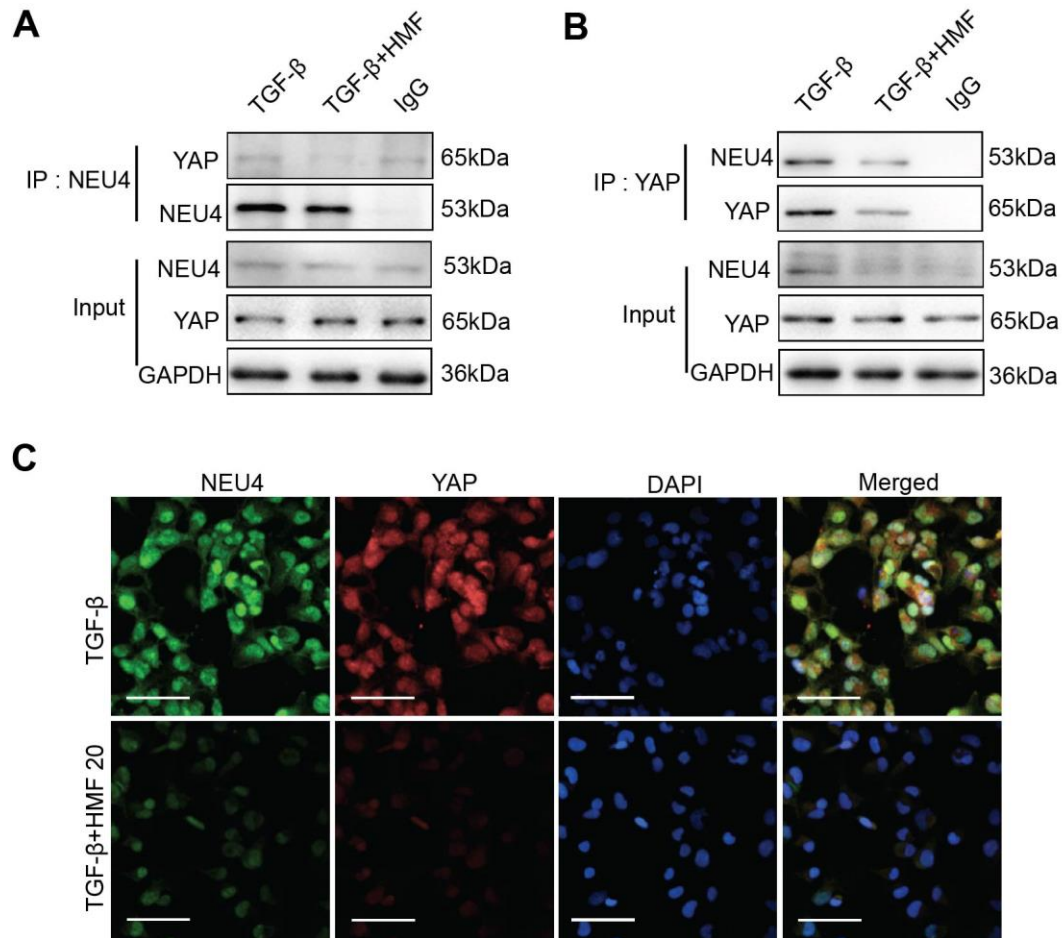
100

101 **Figure S7. NEU4 served as a cellular target of anti-fibrosis small-molecule HMF.**

102 (A) Schematic representation of the HMF molecular capture protocol. (B) Genomes

103 (KEGG) pathway analysis of the identified changed proteins in HK-2 cells 24 h after

104 treatment with TGF- $\beta$ .

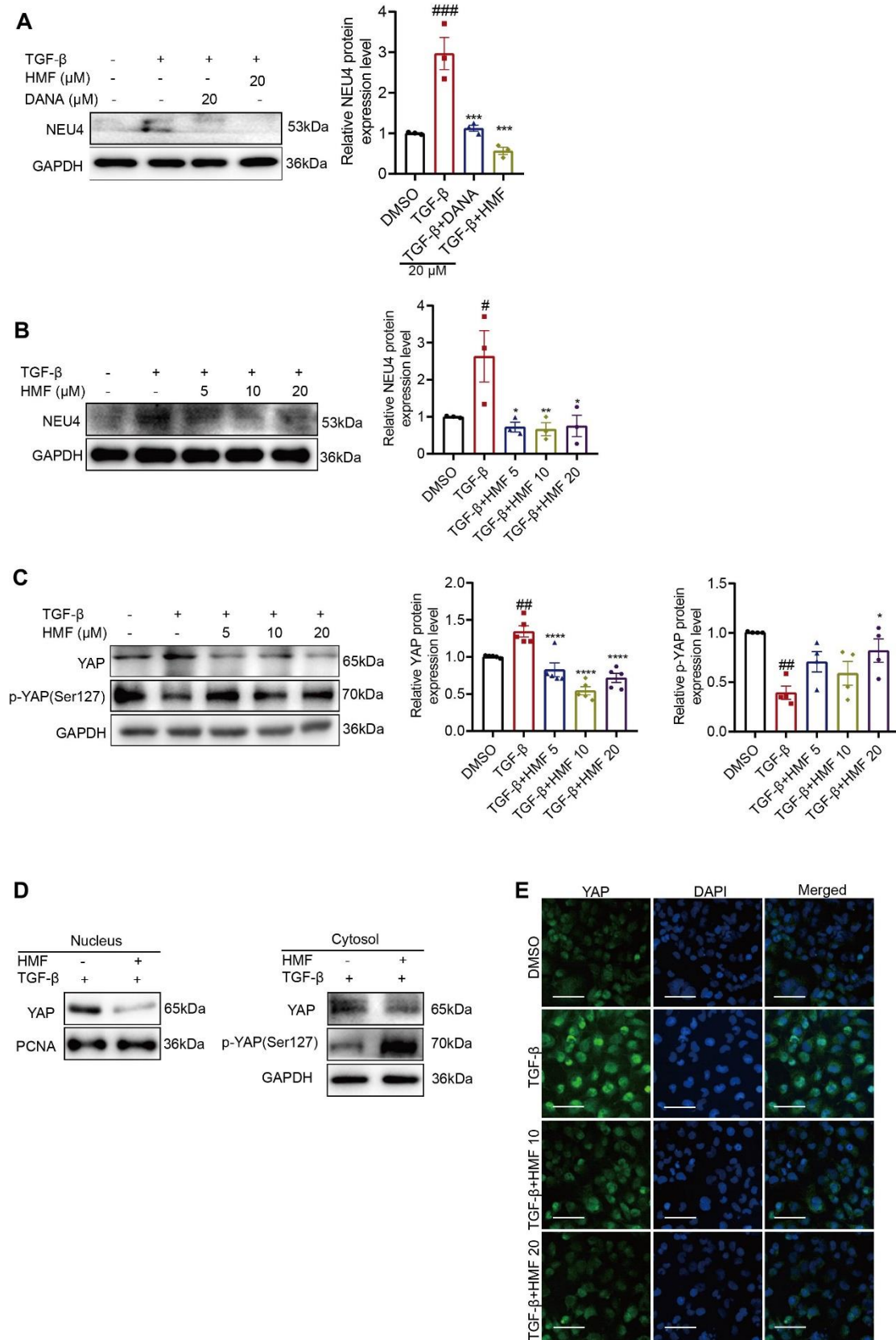


105

106 **Figure S8. HMF inhibited the interaction between NEU4 and YAP. (A and B)**107 Western blotting of CoIP of NEU4 and YAP in HK-2 cells treated with TGF- $\beta$  and in

108 the presence of DMSO or HMF. (C) Colocalization of NEU4 and YAP was analyzed

109 by immunofluorescence in HK-2 cells stimulated with TGF- $\beta$  and in the presence of110 DMSO or HMF 24 h. Scale bar, 100  $\mu$ m,  $n = 3$  samples.



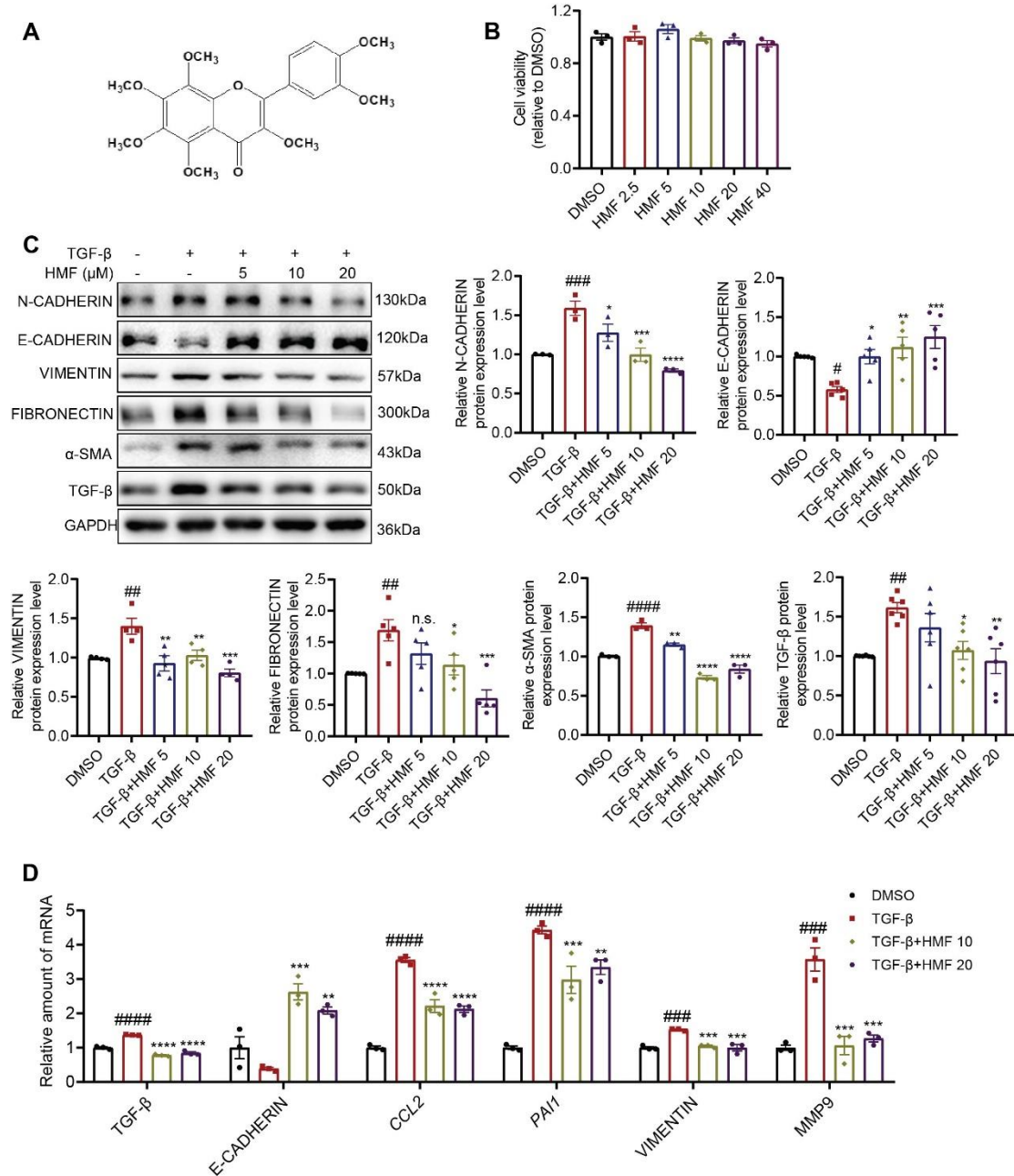
111

112 **Figure S9. HMF inhibited NEU4 and YAP expression.** (A) Western blot (left panel)

113 and quantification (right panel) of the protein expression of NEU4 in HK-2 cells 24 h

114 after treatment with TGF- $\beta$  and in the presence of DANA or HMF. GAPDH served as  
115 loading control,  $n = 3$  samples. **(B and C)** Western blot (left panel) and quantification  
116 (right panel) of the protein expression of NEU4 **(B)**, YAP and phosphorylation of YAP  
117 **(C)** in HK-2 cells 24 h after treatment with TGF- $\beta$  and in the presence of DMSO or  
118 HMF. GAPDH served as loading control,  $n = 3-5$  samples. **(D)** Western blot of the  
119 protein expression of YAP in nuclear and cytosol, phosphorylation of YAP in cytosol in  
120 HK-2 cells 24 h after treatment with TGF- $\beta$  and in the presence of DMSO or HMF. **(E)**  
121 Immunofluorescent staining represents YAP expressions in HK-2 cells treatment with  
122 TGF- $\beta$  and in the presence of DMSO or HMF 24 h. Scale bar, 100  $\mu\text{m}$ ,  $n = 3$  samples.  
123 Error bars represent mean  $\pm$  SEM. Comparisons those among three or more groups by  
124 using one-way analysis of variance (ANOVA) followed by Dunnett's post hoc tests.  
125 \* $p < 0.05$ , \*\* $p < 0.01$ , \*\*\* $p < 0.001$ , \*\*\*\* $p < 0.0001$  versus the TGF- $\beta$  group, # $p < 0.05$ ,  
126 ## $p < 0.01$ , ### $p < 0.001$  versus the DMSO group.

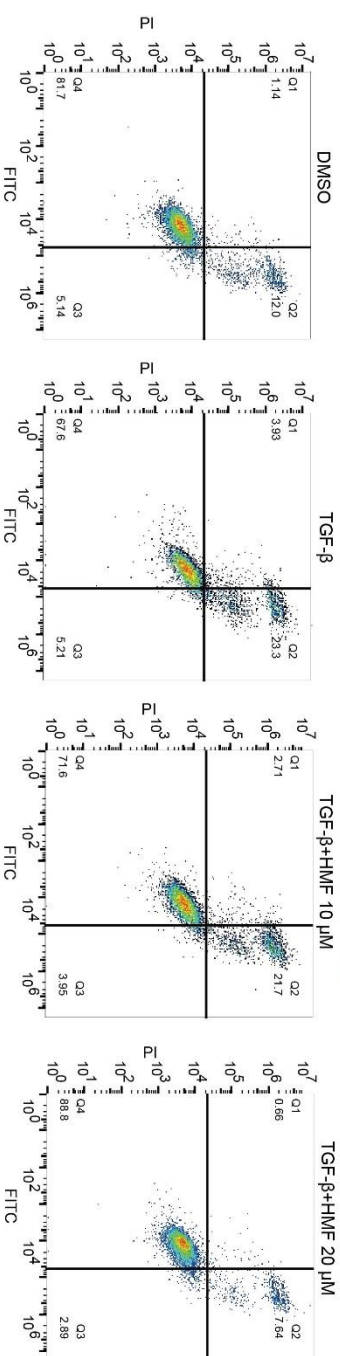
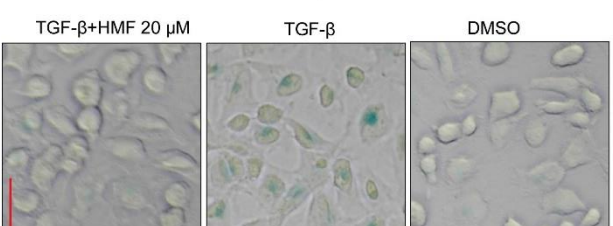
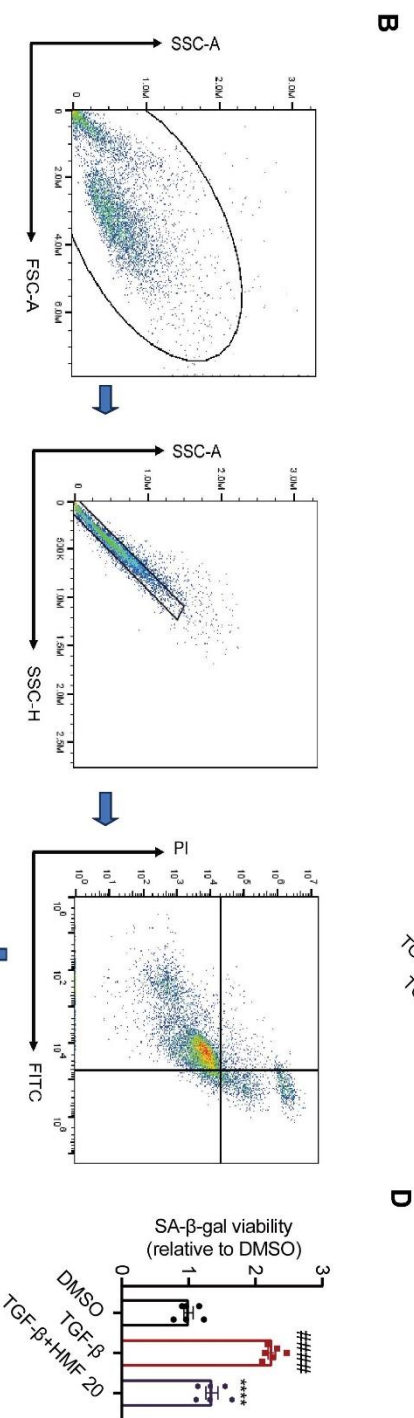
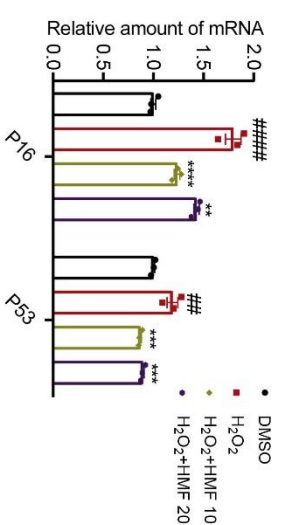
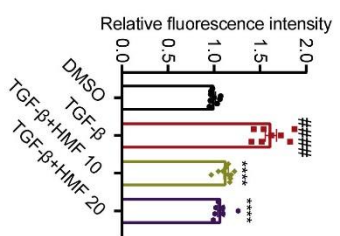
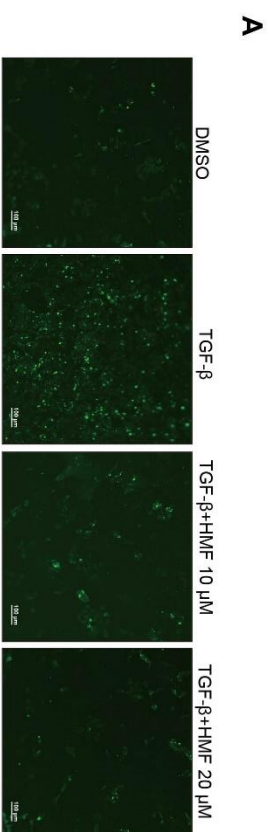
127



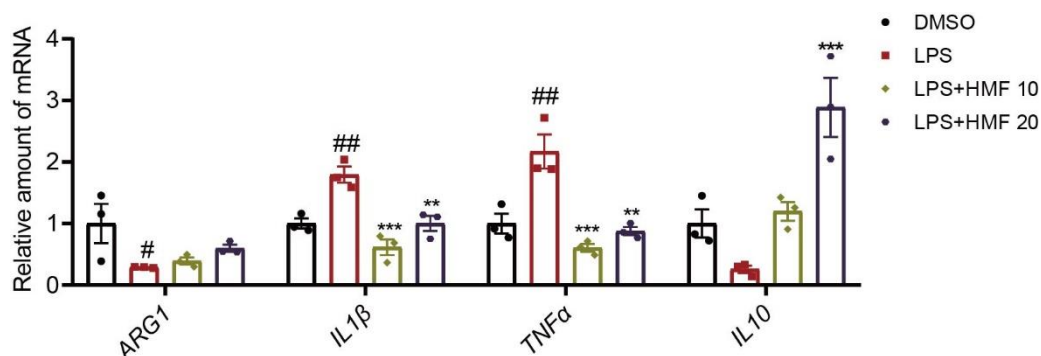
128

129 **Figure S10. HMF inhibited TGF-β-induced EMT, and the production of**  
 130 **proinflammatory cytokines in HK-2. (A) The structure of HMF. (B) Cell viability**  
 131 **after treatment with increasing concentrations of HMF in HK-2 cells for 24 h. *n* = 3**  
 132 **biologically independent samples. (C) Western blot (left panel) and quantification (right**  
 133 **panel) of the protein expression of N-CADHERIN, E-CADHERIN, VIMENTIN,**  
 134 **FIBRONECTIN, α-SMA and TGF-β in HK-2 cells. GAPDH served as loading control.**  
 135 ***n* = 3-6 biologically independent samples. (D) Relative EMT associated gene and**  
 136 **extracellular matrix associated gene mRNA level in HK-2 cells. *n* = 3 biologically**

137 independent samples. (C and D) HK-2 cells treated with TGF- $\beta$  and in the presence of  
138 DMSO or HMF for 24 h. Error bars represent mean  $\pm$  SEM. Comparisons those among  
139 three or more groups by using one-way analysis of variance (ANOVA) followed by  
140 Dunnett's post hoc tests. \* $p$ <0.05, \*\* $p$ <0.01, \*\*\* $p$ <0.001, \*\*\*\* $p$ <0.0001 versus the  
141 TGF- $\beta$  group, # $p$ <0.05, ## $p$ <0.001, ### $p$ <0.001, #### $p$ <0.0001 versus the DMSO group.

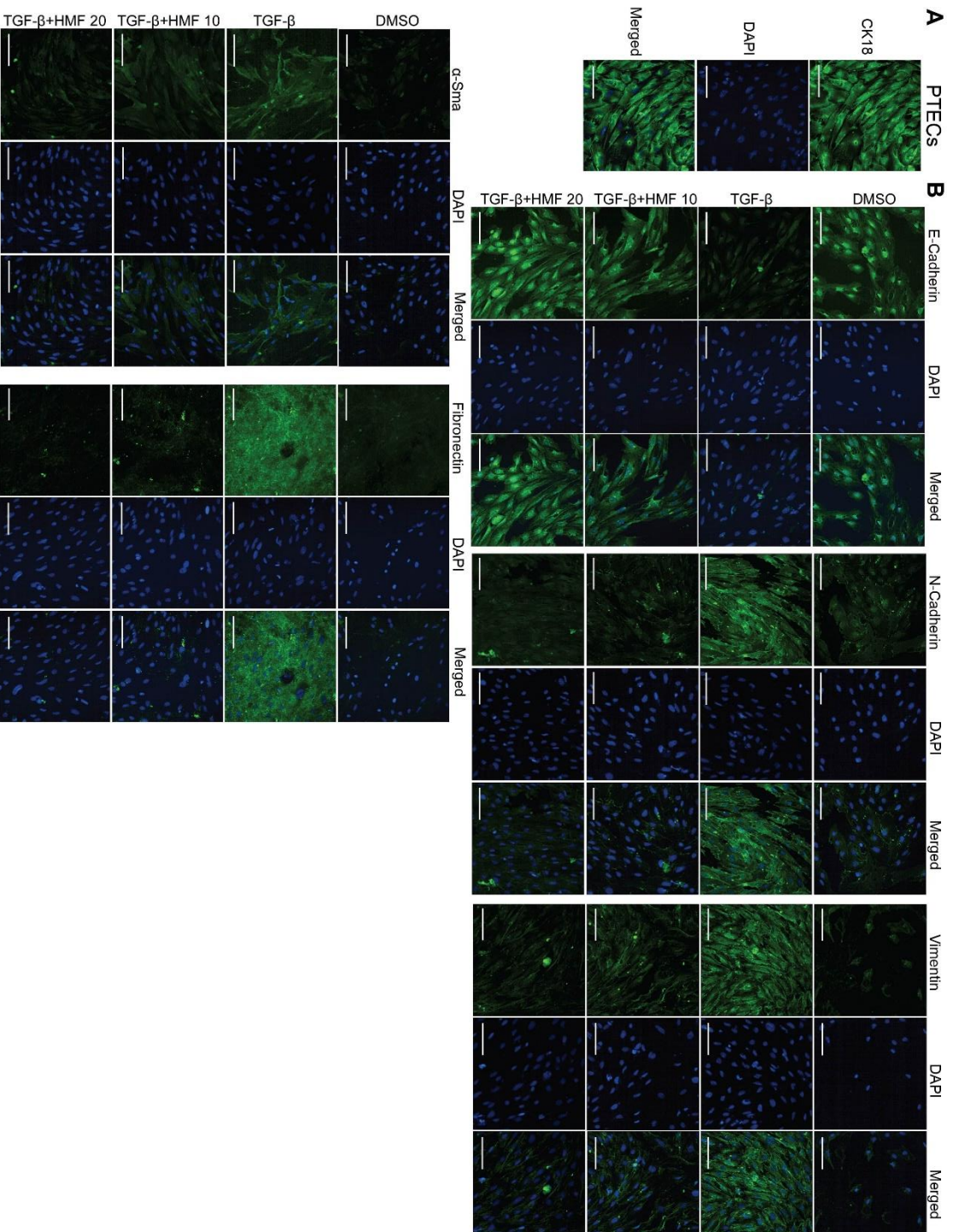


143 **Figure S11. HMF ameliorated TGF- $\beta$ -induced apoptosis and cellular senescence**  
144 **in HK-2.** (A) Measurement (left panel) and the quantification (right panel) of apoptosis  
145 by TUNEL staining in HK-2 cells. Scale bar, 100  $\mu$ m.  $n = 10$  samples. (B) Measurement  
146 of apoptosis by flow cytometric analysis in HK-2 cells. (C) Relative senescence  
147 associated gene mRNA level in HK-2 cells after treatment with H<sub>2</sub>O<sub>2</sub> in the presence  
148 of DMSO or HMF,  $n = 3$  biologically independent samples. (D) Measurement (right  
149 panel) and the quantification (left panel) of SA- $\beta$ -gal activity by SA- $\beta$ -gal staining in  
150 HK-2 cells. Scale bar, 100  $\mu$ m.  $n = 6$  samples. (A, B and D) HK-2 cells treated with  
151 TGF- $\beta$  and in the presence of DMSO or HMF for 24 h. Error bars represent mean  $\pm$   
152 SEM. Comparisons those among three or more groups by using one-way analysis of  
153 variance (ANOVA) followed by Dunnett's post hoc tests. \*\* $p < 0.01$ , \*\*\* $p < 0.001$ ,  
154 \*\*\*\* $p < 0.0001$  versus the TGF- $\beta$  or H<sub>2</sub>O<sub>2</sub> group, ## $p < 0.01$ , ##### $p < 0.0001$  versus the  
155 DMSO group.  
156

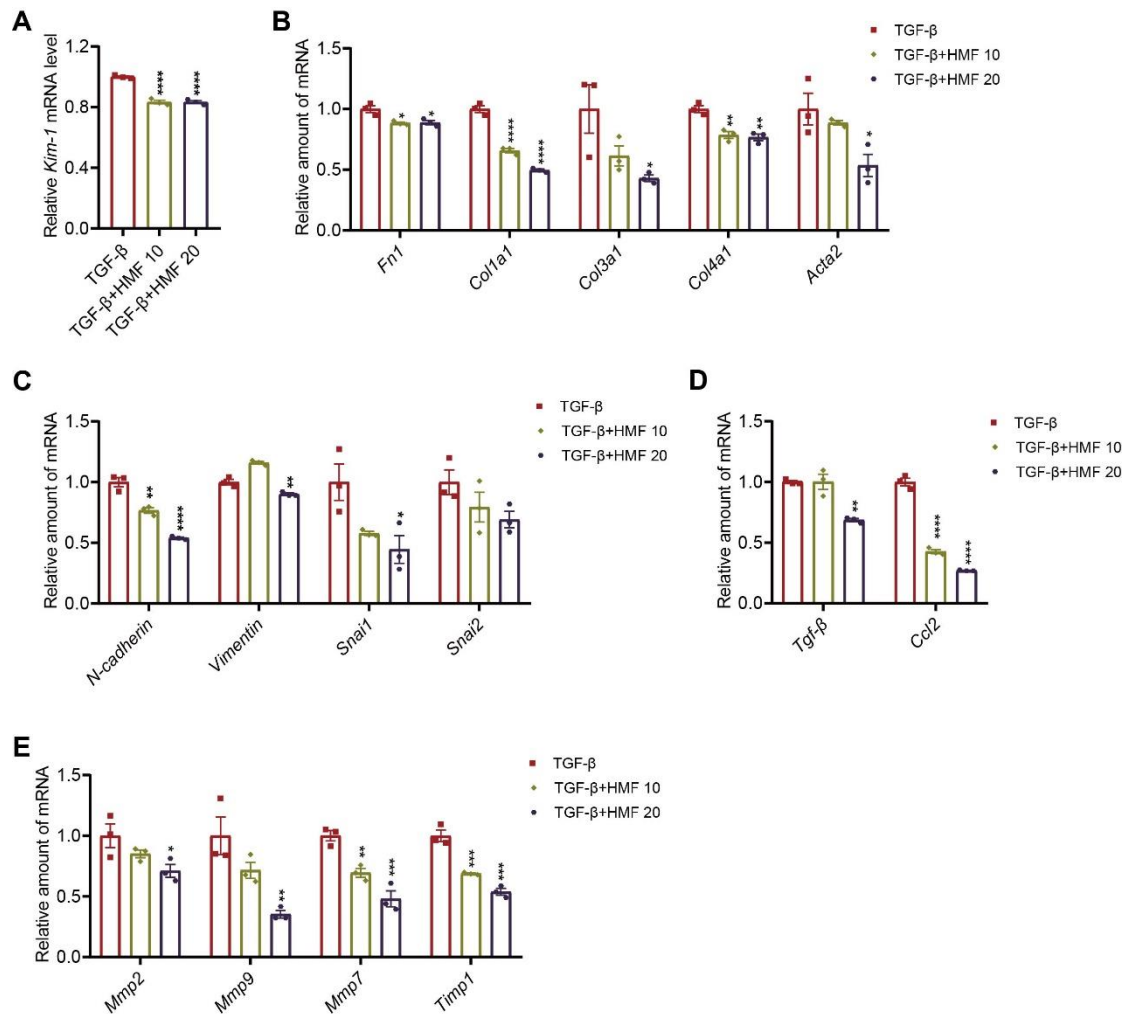


157

158 **Figure S12. HMF inhibited LPS-induced inflammation in HK-2.** Relative  
 159 inflammation associated gene mRNA level in HK-2 cells 24 h after treatment with LPS  
 160 in the presence of DMSO or HMF,  $n = 3$  biologically independent samples. Error bars  
 161 represent mean  $\pm$  SEM. Comparisons those among three or more groups by using one-  
 162 way analysis of variance (ANOVA) followed by Dunnett's post hoc tests. \*\* $p < 0.01$ ,  
 163 \*\*\* $p < 0.001$  versus the LPS group, # $p < 0.05$ , ## $p < 0.01$  versus the DMSO group.

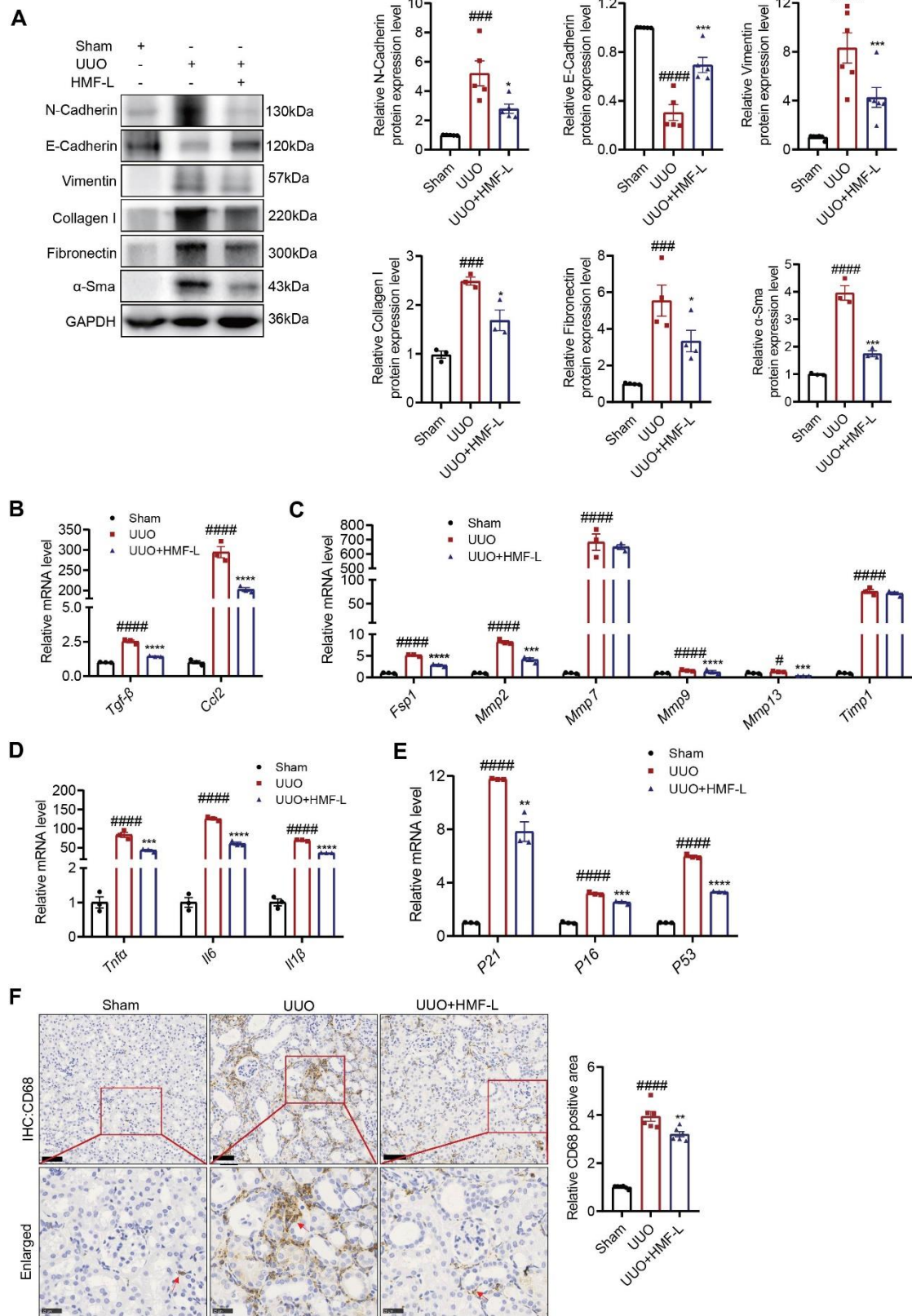


165 **Figure S13. HMF inhibited TGF- $\beta$ -induced EMT in PTECs. (A)**  
166 Immunofluorescent staining represents CK18 expressions in PTECs. Scale bar, 100  $\mu\text{m}$ ,  
167  $n = 3$  samples. **(B)** Immunofluorescent staining represents N-Cadherin, E-Cadherin,  
168 Vimentin,  $\alpha$ -Sma and Fibronectin expressions in PTECs 24 h after treatment with TGF-  
169  $\beta$  and in the presence of DMSO or HMF. Scale bar, 100  $\mu\text{m}$ ,  $n = 3$  samples.  
170



171

172 **Figure S14. HMF inhibited TGF- $\beta$ -induced EMT, and the production of**  
 173 **proinflammatory cytokines in PTECs. (A-E) PTECs treated with TGF- $\beta$  and in the**  
 174 **presence of DMSO or HMF for 24 h. (A) *Kim-1* mRNA level in PTECs,  $n = 3$**   
 175 **biologically independent samples. (B-E) Relative ECM associated gene (B), EMT**  
 176 **associated gene (C), chemokine associated gene (D), and extracellular matrix**  
 177 **associated gene (E) mRNA level in PTECs,  $n = 3$  biologically independent samples.**  
 178 **Error bars represent mean  $\pm$  SEM. Comparisons those among three or more groups by**  
 179 **using one-way analysis of variance (ANOVA) followed by Dunnett's post hoc tests.**  
 180 **\* $p < 0.05$ , \*\* $p < 0.01$ , \*\*\* $p < 0.001$ , \*\*\*\* $p < 0.0001$  versus the TGF- $\beta$  group.**

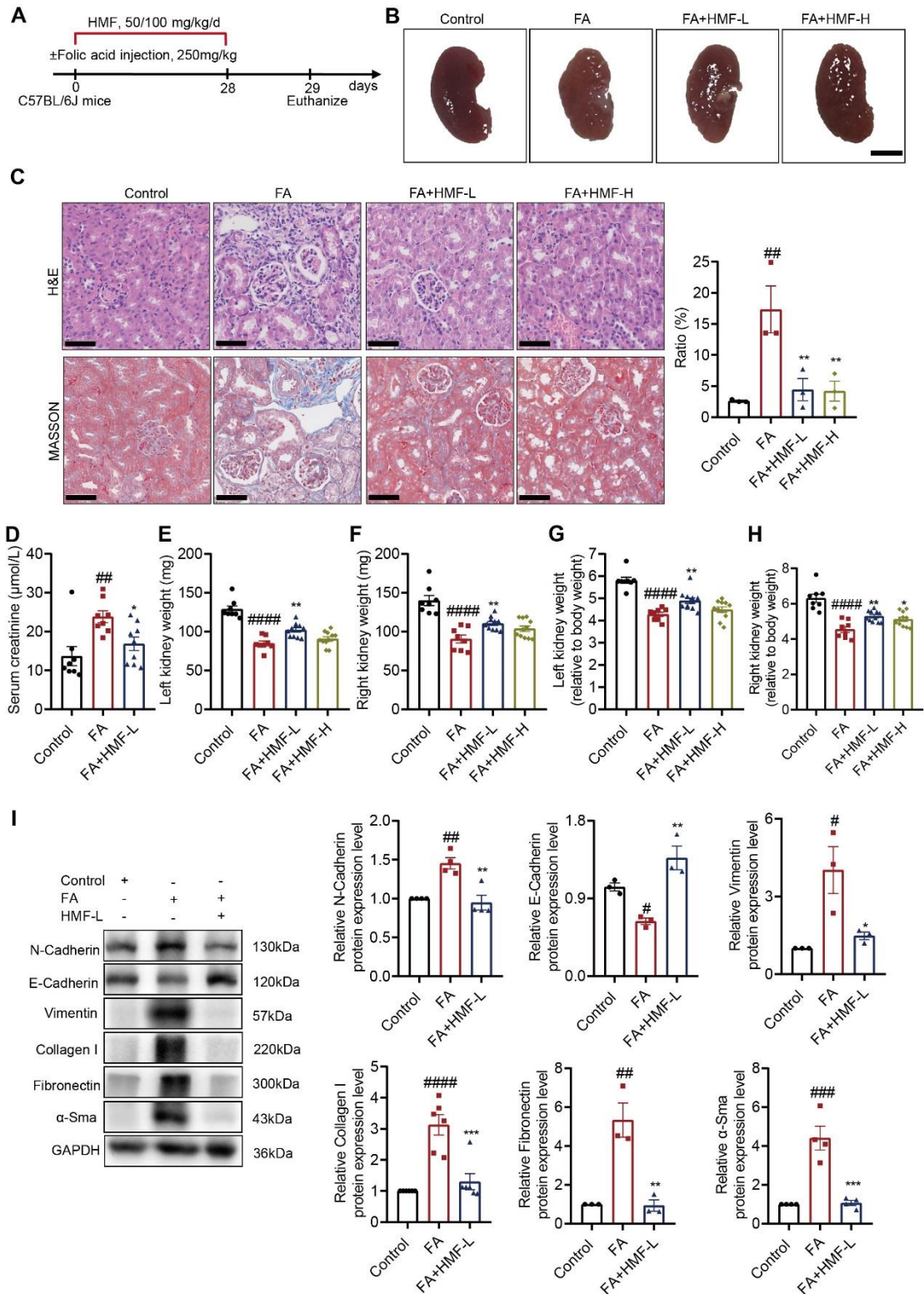


181

182 **Figure S15. HMF improved UUO-induced renal fibrosis in mice.** Vehicle, or HMF

183 (50 or 100 mg/kg/day) was administrated to UUO mice by gastric irrigation once daily

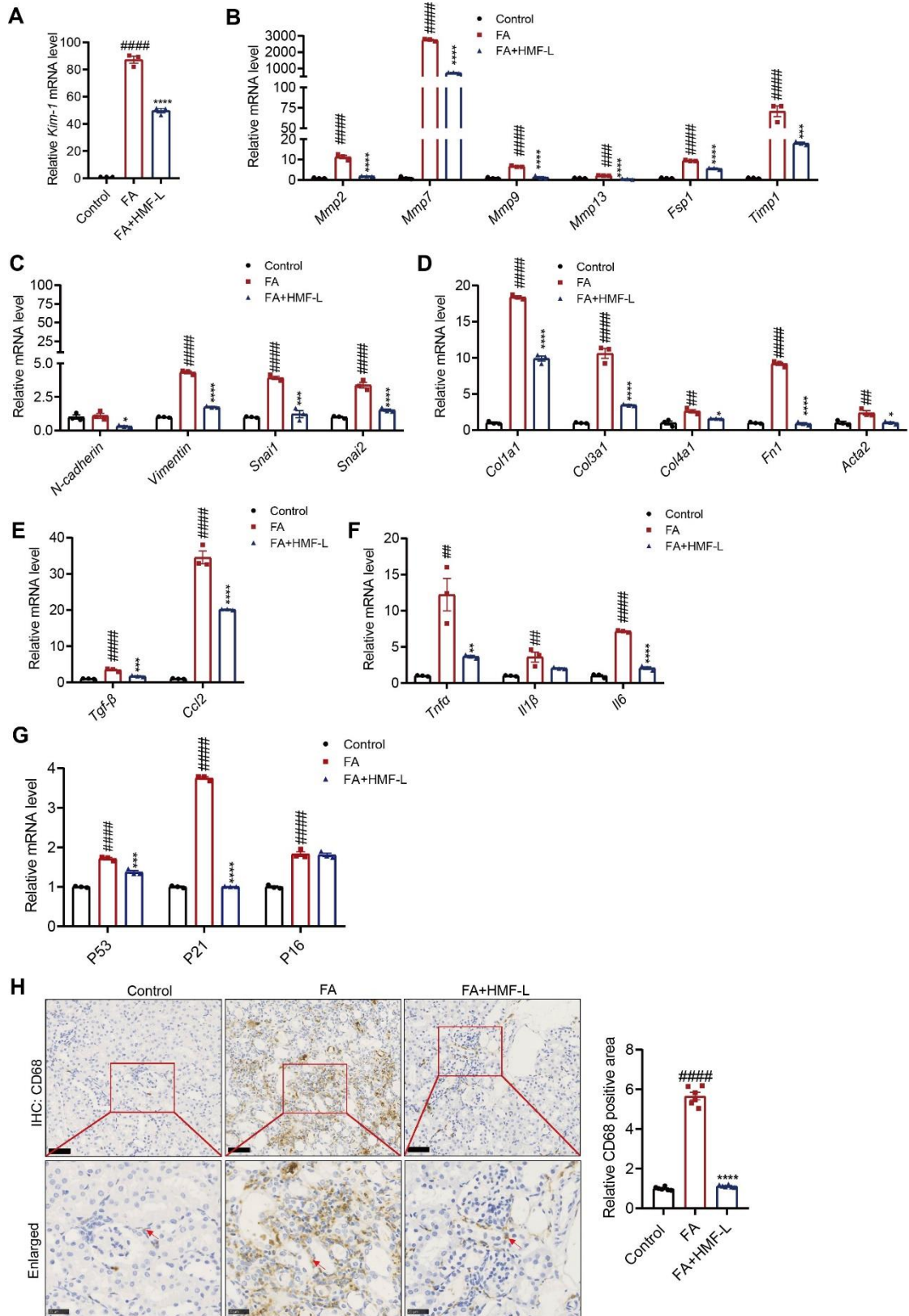
184 for 10 days. UUO, unilateral ureteral obstruction. (A) Western blot (left panel) and  
185 quantification (right panel) of the protein expression of N-Cadherin, E-Cadherin,  
186 Vimentin, Collagen I, Fibronectin and  $\alpha$ -Sma in left kidneys, GAPDH served as loading  
187 control,  $n = 3-6$  mice. (B-E) Relative mRNA level of chemokine-associated genes (B),  
188 extracellular matrix-associated genes (C), inflammation associated genes (D) and  
189 senescence-associated genes (E) were determined by RT-qPCR from left kidneys.  $n =$   
190 3 biologically independent samples. (F) Immunohistochemistry staining analysis (left  
191 panel) and quantification (right panel) of CD68 expression in left kidney tissues,  $n = 6$   
192 mice. Scale bar, 50  $\mu\text{m}$ . Error bars represent mean  $\pm$  SEM. Comparisons those among  
193 three or more groups by using one-way analysis of variance (ANOVA) followed by  
194 Dunnett's post hoc tests. \* $p < 0.05$ , \*\* $p < 0.01$ , \*\*\* $p < 0.001$ , \*\*\*\* $p < 0.0001$  versus the  
195 UUO group, ### $p < 0.001$ , #### $p < 0.0001$  versus the Sham group.  
196



197

198 **Figure S16. HMF ameliorated FA-induced renal fibrosis in mice.** The mice were  
 199 intraperitoneally injected with folic acid (250 mg/kg). Vehicle, or HMF (50 or 100  
 200 mg/kg/day) was administrated to folic acid mice by gastric irrigation once daily for 28  
 201 days. (A) Scheme of the experimental approach. (B) Representative picture of left

202 kidneys of mice with different treatments. (C) Representative photomicrographs of the  
203 H&E staining and Masson's trichrome staining from left kidneys, renal interstitial  
204 fibrosis scores based on Masson's trichrome staining (right panel),  $n = 3$  mice. Scale  
205 bar, 50  $\mu\text{m}$ . (D) Creatinine in serum,  $n = 8-11$  mice. (E and F) The left (E) and right (F)  
206 renal weight. (G and H) The ratio of left (G) and right (H) renal weight to body weight  
207 (BW),  $n = 8-11$  mice. (I) Western blot (left panel) and quantification (right panel) of the  
208 protein expression of N-Cadherin, E-Cadherin, Vimentin, Collagen I, Fibronectin and  
209  $\alpha$ -Sma in left kidneys, GAPDH served as loading control,  $n = 3-6$  mice. Error bars  
210 represent mean  $\pm$  SEM. Comparisons those among three or more groups by using one-  
211 way analysis of variance (ANOVA) followed by Dunnett's post hoc tests.  $*p < 0.05$ ,  
212  $**p < 0.01$ ,  $***p < 0.001$  versus the FA group,  $^{\#}p < 0.05$ ,  $^{\#\#}p < 0.01$ ,  $^{\#\#\#}p < 0.001$ ,  
213  $^{\#\#\#\#}p < 0.0001$  versus the Control group.



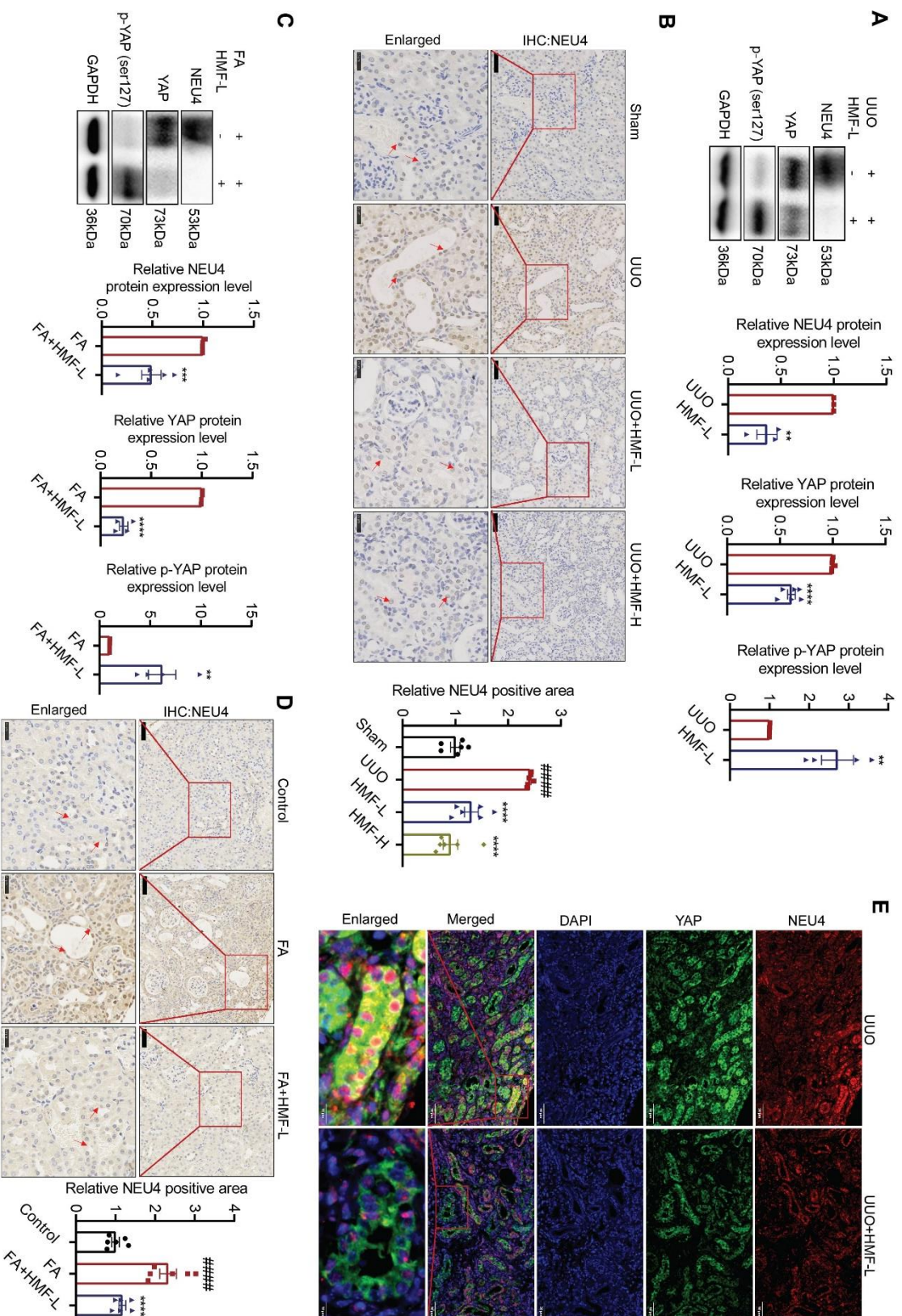
214

215

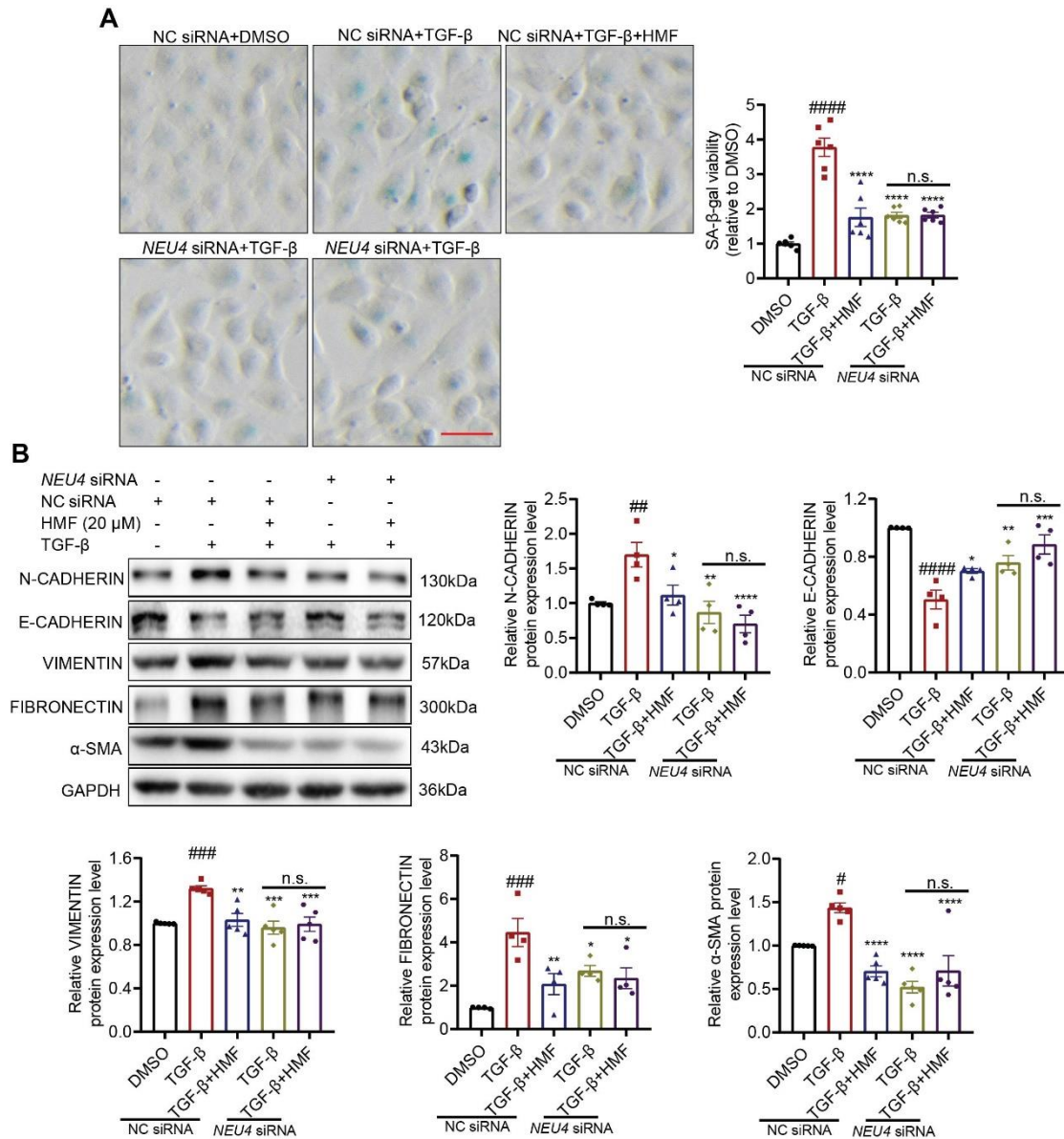
216

**Figure S17. HMF inhibited FA-induced EMT, the production of proinflammatory cytokines, and macrophage infiltration in mice. The mice were intraperitoneally**

217 injected with folic acid (250 mg/kg). Vehicle, or HMF (50 or 100 mg/kg/day) was  
218 administrated to folic acid mice by gastric irrigation once daily for 28 days. (A) *Kim-1*  
219 mRNA level in left kidneys,  $n = 3$  mice. (B-G) Relative extracellular matrix associated  
220 gene (B), EMT associated gene (C), ECM associated gene (D), chemokine associated  
221 gene (E), inflammation associated gene (F) and senescence-associated genes (G)  
222 mRNA level in left kidneys,  $n = 3$  mice. (H) Immunohistochemistry staining analysis  
223 (left panel) and quantification (right panel) of CD68 expression in kidney tissues,  $n = 6$   
224 mice. Scale bar, 50  $\mu\text{m}$ . Error bars represent mean  $\pm$  SEM. Comparisons those among  
225 three or more groups by using one-way analysis of variance (ANOVA) followed by  
226 Dunnett's post hoc tests. \* $p < 0.05$ , \*\* $p < 0.01$ , \*\*\* $p < 0.001$ , \*\*\*\* $p < 0.0001$  versus the FA  
227 group, ## $p < 0.01$ , ### $p < 0.001$ , #### $p < 0.0001$  versus the Control group.



229 **Figure S18. HMF inhibited the interaction between NEU4 with YAP, and**  
230 **activation of YAP in UUO or folic acid-induced mice. (A)** Western blot (left panel)  
231 and quantification (right panel) of the protein expression of NEU4, YAP and  
232 phosphorylation of YAP in left kidneys. GAPDH served as loading control,  $n = 3-5$   
233 mice. **(B)** Immunohistochemistry staining analysis (left panel) and quantification (right  
234 panel) of NEU4 in left kidney tissues.  $n = 6$  mice. Scale bar, 50  $\mu\text{m}$ . **(C)** Western blot  
235 (left panel) and quantification (right panel) of the protein expression of NEU4, YAP and  
236 phosphorylation of YAP in kidneys. GAPDH served as loading control,  $n = 3-5$  mice.  
237 **(D)** Immunohistochemistry staining analysis (left panel) and quantification (right panel)  
238 of NEU4 in kidney tissues.  $n = 6$  mice. Scale bar, 50  $\mu\text{m}$ . **(E)** Colocalization of NEU4  
239 and YAP was analyzed by immunofluorescence in left kidneys. Scale bar, 50  $\mu\text{m}$ .  $n = 6$   
240 mice. **(A, B and E)** Vehicle, or HMF (50 or 100 mg/kg/day) was administrated to UUO  
241 mice by gastric irrigation once daily for 10 days. **(C and D)** The mice were  
242 intraperitoneally injected with folic acid (250 mg/kg). Vehicle, or HMF (50 or 100  
243 mg/kg/day) was administrated to folic acid mice by gastric irrigation once daily for 28  
244 days. Error bars represent mean  $\pm$  SEM. Comparisons between two groups were  
245 analyzed by using a two-tailed Student's  $t$  test. Comparisons those among three or more  
246 groups by using one-way analysis of variance (ANOVA) followed by Dunnett's post  
247 hoc tests. \*\* $p < 0.01$ , \*\*\* $p < 0.001$ , \*\*\*\* $p < 0.0001$  versus the UUO or FA group,  
248 ##### $p < 0.0001$  versus the Sham or Control group.



249

250 **Figure S19. NEU4 knockdown abolished the anti-fibrotic effect of HMF in HK-2.**

251 HK-2 cells treatment with TGF-β and in the presence of DMSO or HMF 24 h after

252 transfection with *NEU4* siRNA. (A) Measurement (left panel) and quantification (right

253 panel) of SA-β-gal activity by SA-β-gal staining in HK-2 cells, *n* = 6 biologically

254 independent samples. Scale bar, 100 μm. (B) Western blot (left panel) and quantification

255 (right panel and bottom panel) of the protein expression of N-CADHERIN, E-

256 CADHERIN, VIMENTIN, FIBRONECTIN and α-SMA in HK-2 cells. GAPDH served

257 as loading control. *n* = 4-5 biologically independent samples. Error bars represent mean

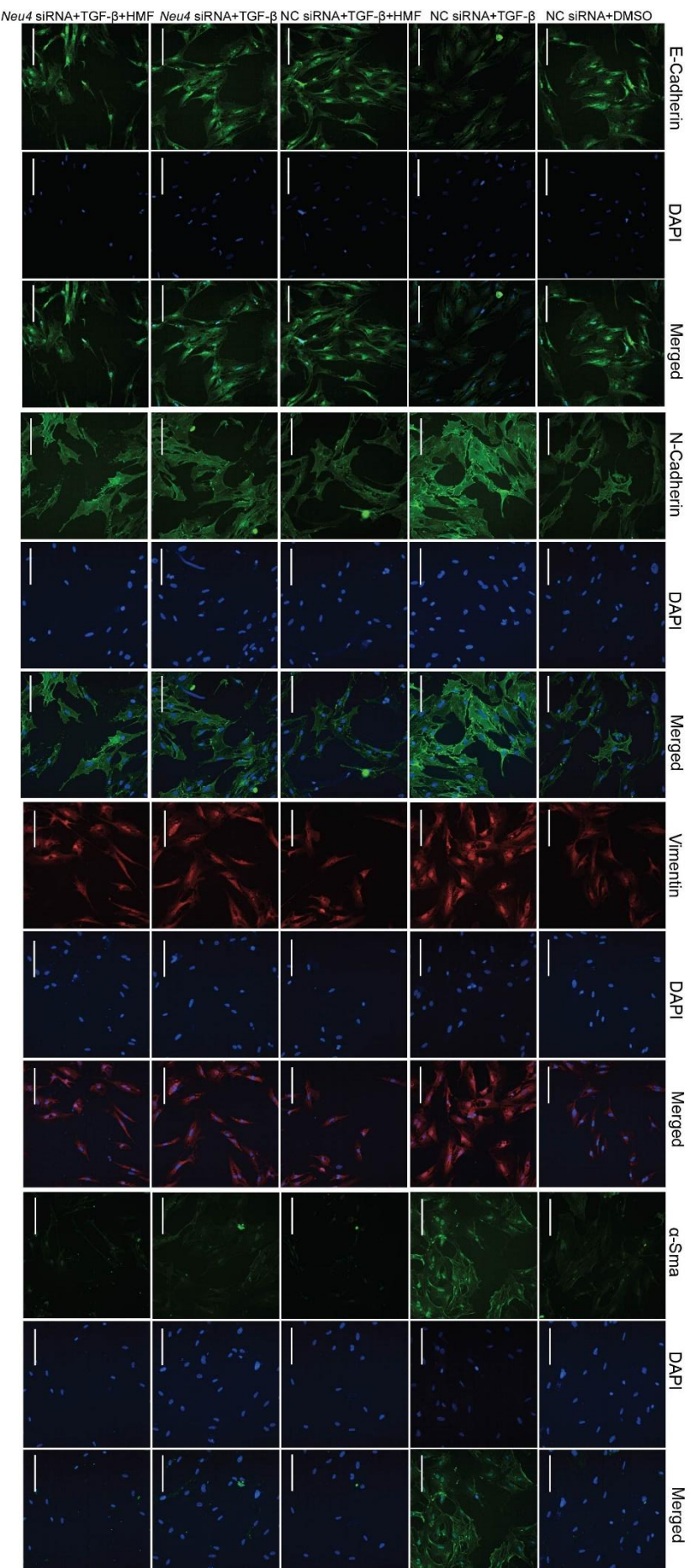
258 ± SEM. Comparisons those among three or more groups by using one-way analysis of

259 variance (ANOVA) followed by Dunnett's post hoc tests. \**p*<0.05, \*\**p*<0.01,

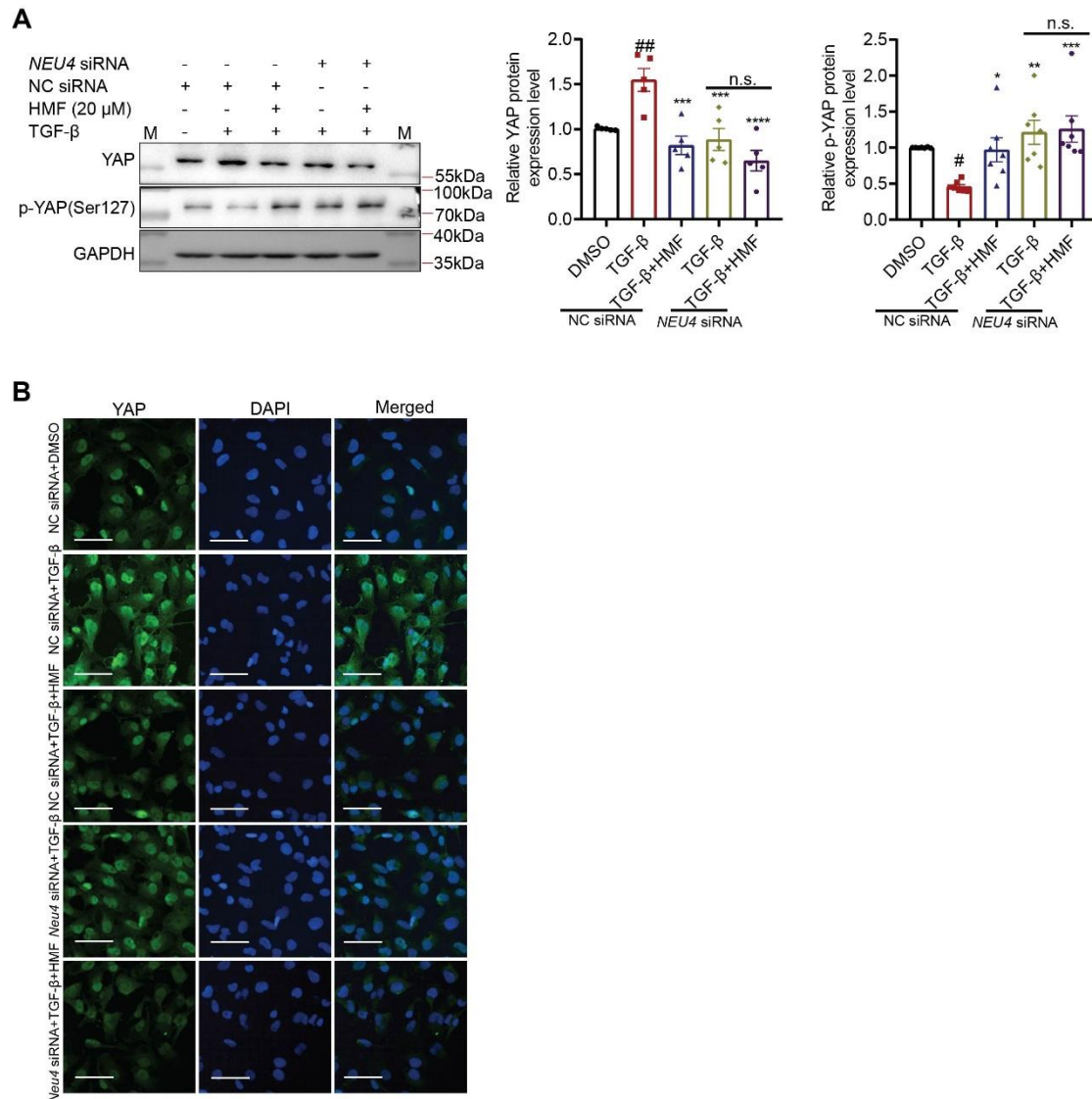
260 \*\*\* $p < 0.001$ , \*\*\*\* $p < 0.0001$  versus the NC siRNA+TGF- $\beta$  group, # $p < 0.05$ , ## $p < 0.01$ ,

261 ### $p < 0.001$ , #### $p < 0.0001$  versus the NC siRNA+DMSO group. n.s.: no significance.

262

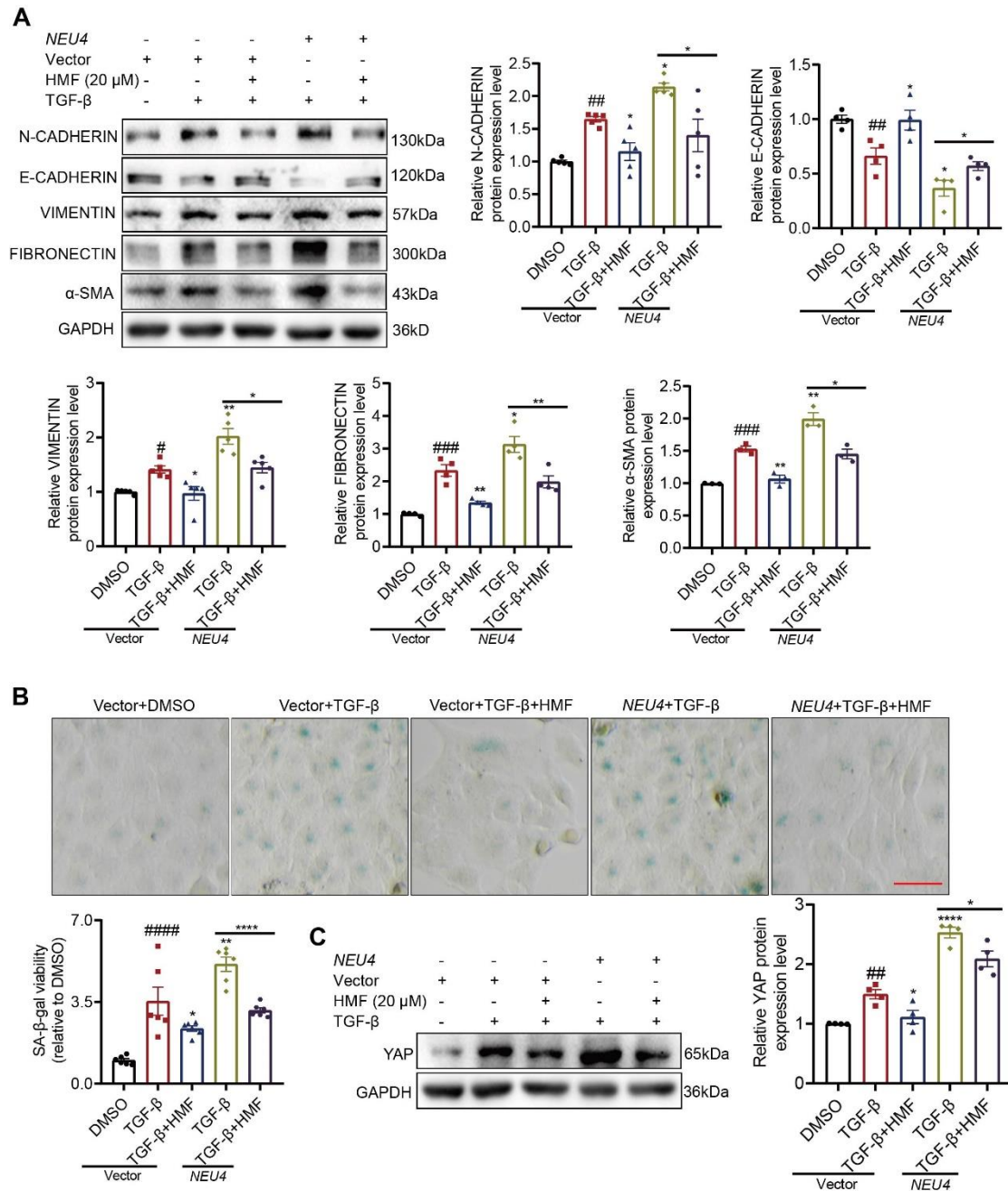


263  
 264 **Figure S20. Knockdown of NEU4 abolished the anti-fibrotic effect of HMF in PTECs.** Immunofluorescent staining represents N-Cadherin,  
 265 E-Cadherin, Vimentin and  $\alpha$ -Sma expressions in PTECs treatment with TGF- $\beta$  and in the presence of DMSO or HMF 24 h after transfection with  
 266 *NEU4* siRNA.  $n = 3$  biologically independent samples. Scale bar, 100  $\mu$ m.



267

268 **Figure S21. NEU4 knockdown abolished the downregulation of YAP by HMF. HK-**269 **2 cells treatment with TGF- $\beta$  and in the presence of DMSO or HMF 24 h after**270 **transfection with *NEU4* siRNA. (A) Western blot (left panel) and quantification (right**271 **panel) of the protein expression of YAP and phosphorylation of YAP in HK-2 cells.**272 **GAPDH served as loading control.  $n = 5-7$  biologically independent samples. M,**273 **Marker. (B) Immunofluorescent staining represents YAP expressions in HK-2 cells**274 **treatment with TGF- $\beta$  and in the presence of DMSO or HMF 24 h after transfection**275 **with *NEU4* siRNA. Scale bar, 100  $\mu$ m,  $n = 3$  samples. Error bars represent mean  $\pm$  SEM.**276 **Comparisons those among three or more groups by using one-way analysis of variance**277 **(ANOVA) followed by Dunnett's post hoc tests. \* $p < 0.05$ , \*\* $p < 0.01$ , \*\*\* $p < 0.001$ ,**278 **\*\*\*\* $p < 0.0001$  versus the NC siRNA+TGF- $\beta$  group, # $p < 0.05$ , ## $p < 0.001$  versus the NC**279 **siRNA+DMSO group. n.s.: no significance.**

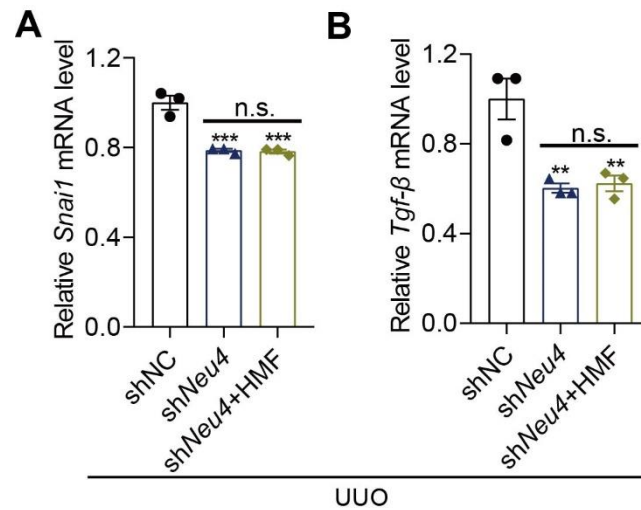


280

281 **Figure S22. HMF ameliorated TGF- $\beta$ -induced EMT and cellular senescence is**  
 282 **dependent on NEU4 in HK-2.** HK-2 cells treated with TGF- $\beta$  and in the presence of  
 283 DMSO or HMF 24 h after transfection with *NEU4*-overexpression plasmids. (A)  
 284 Western blot (left panel) and quantification (right panel and bottom panel) of the protein  
 285 expression of N-CADHERIN, E-CADHERIN, VIMENTIN, FIBRONECTIN and  $\alpha$ -  
 286 SMA in HK-2 cells. GAPDH served as loading control.  $n = 3-6$  biologically  
 287 independent samples. (B) Measurement (top panel) and the quantification (bottom  
 288 panel) of SA- $\beta$ -gal activity by SA- $\beta$ -gal staining in HK-2 cells.  $n = 6$  biologically

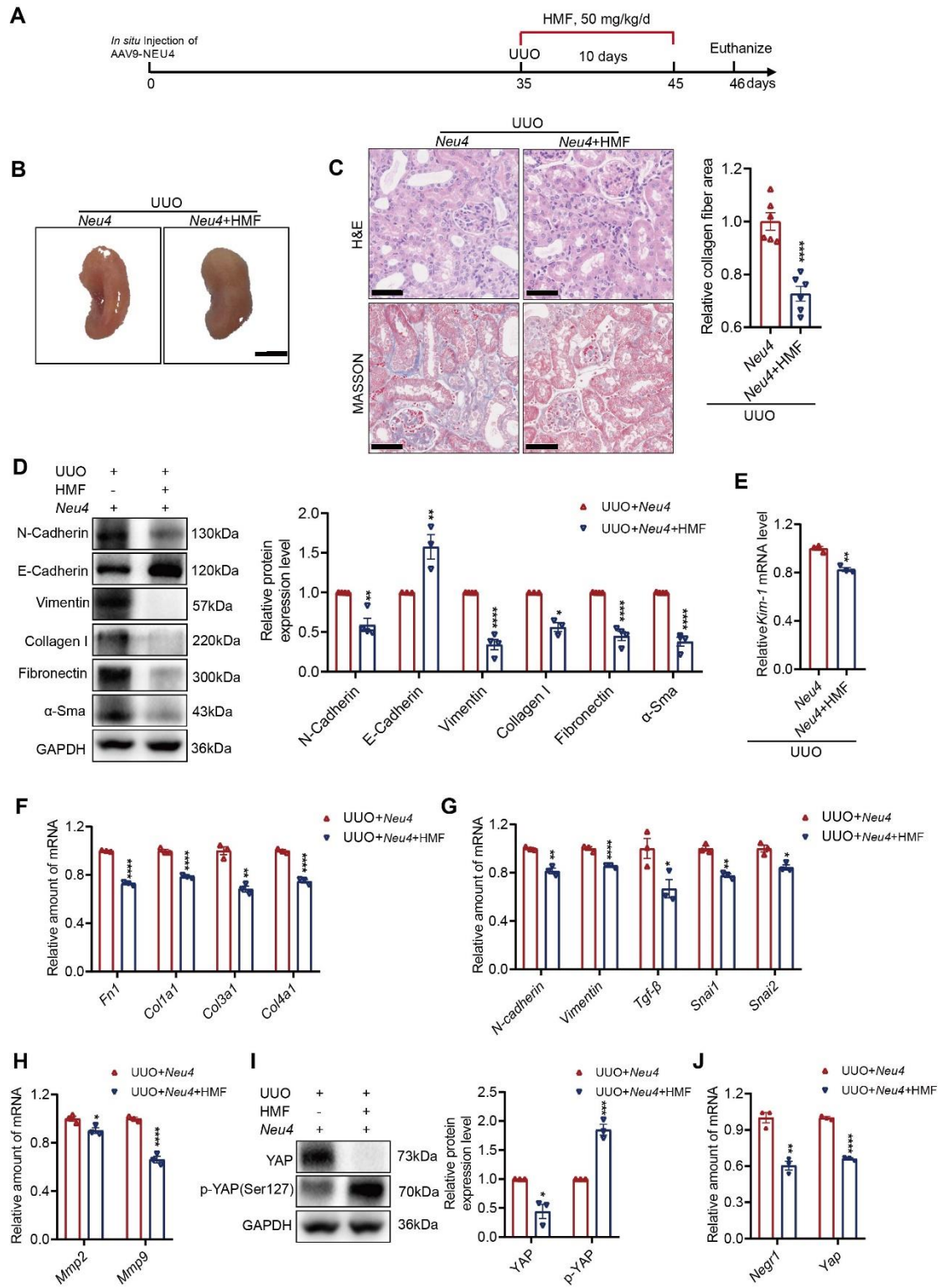
289 independent samples. Scale bar, 100  $\mu\text{m}$ . (C) Western blot (left panel) and  
290 quantification (right panel) of the protein expression of YAP in HK-2 cells, GAPDH  
291 served as loading control,  $n = 4$  biologically independent samples. Error bars represent  
292 mean  $\pm$  SEM. Comparisons those among three or more groups by using one-way  
293 analysis of variance (ANOVA) followed by Dunnett's post hoc tests. \* $p < 0.05$ , \*\* $p < 0.01$ ,  
294 \*\*\*\* $p < 0.0001$  versus the Vector+TGF- $\beta$  or *NEU4*+TGF- $\beta$  group, # $p < 0.05$ , ## $p < 0.001$ ,  
295 ### $p < 0.01$ , #### $p < 0.0001$  versus the Vector+DMSO group.

296



297

298 **Figure S23. *Neu4* knockdown relieved *Snai1* and *Tgf-β* inhibition effect of HMF in**  
 299 **UUO model.** Six-week-old male C57BL/6J mice were injected with shNC or sh*Neu4*  
 300 adenoviruses. Five weeks after injection, the mice were subjected to UUO surgery, then  
 301 vehicle or HMF (50 mg/kg/day) was administrated to mice by gastric irrigation once  
 302 daily for 10 days. (A and B) Relative EMT associated gene mRNA level in left kidneys,  
 303  $n = 3$  mice. Error bars represent mean  $\pm$  SEM. Comparisons those among three or more  
 304 groups by using one-way analysis of variance (ANOVA) followed by Dunnett's post  
 305 hoc tests. \*\* $p < 0.01$ , \*\*\* $p < 0.001$  versus the shNC group. n.s.: no significance.



306

307

308

309

310

**Figure S24. Relief of renal fibrosis by HMF was dependent on NEU4.** Mice was *in situ* injected with AAV9 encoding GFP-*Neu4*. Five weeks after injection, the mice were subjected to UUU surgery, then vehicle or HMF (50 mg/kg/day) was administrated to mice by gastric irrigation once daily for 10 days. (A) The schematic of experimental

311 design. **(B)** Representative picture of left kidneys of UUO mice. Scale bar, 100  $\mu\text{m}$ ,  $n$   
312 = 3 mice. **(C)** Representative photomicrographs of the H&E staining and Masson's  
313 trichrome staining from left kidneys of UUO mice (left panel), and renal interstitial  
314 fibrosis scores based on Masson's trichrome staining (right panel).  $n = 6$  mice. H&E  
315 staining, scale bar, 50  $\mu\text{m}$ . Masson's trichrome staining, scale bar, 100  $\mu\text{m}$ . **(D)** Western  
316 blot (left panel) and quantification (right panel) of the protein expression of N-Cadherin,  
317 E-Cadherin, Vimentin, Collagen I, Fibronectin and  $\alpha$ -Sma in kidneys, GAPDH served  
318 as loading control.  $n = 3$ -4 mice. **(E)** *Kim-1* gene mRNA level in left kidneys.  $n = 3$   
319 mice. **(F-H)** Relative ECM associated gene **(F)**, EMT associated gene **(G)**, extracellular  
320 matrix associated gene **(H)** mRNA level in left kidneys.  $n = 3$  mice. **(I)** Western blot  
321 (left panel) and quantification (right panel) of the protein expression of YAP and  
322 phosphorylation of YAP in kidneys. GAPDH served as loading control,  $n = 3$  mice. **(J)**  
323 Relative mRNA abundance of *Yap* target genes in left kidney tissue,  $n = 3$  mice. Error  
324 bars represent mean  $\pm$  SEM. Comparisons between two groups were analyzed by using  
325 a two-tailed Student's *t* test. \* $p < 0.05$ , \*\* $p < 0.01$ , \*\*\* $p < 0.001$ , \*\*\*\* $p < 0.0001$  versus the  
326 *Neu4* group.